

Fisken og Havet, nummer 14 - 2001

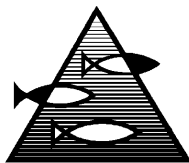
**Potential implications on the pelagic fish and
zooplanton community of artificially induced
deep-water releases of oil and gas during
DeepSpill_2000 --- an innovative acoustic approach**

Tor Knutsen and Bjørn Serigstad



 **HAVFORSKNINGSINSTITUTTET**
INSTITUTE OF MARINE RESEARCH

PROSJEKTRAPPORT



ISSN 0071-5638

HAVFORSKNINGSINSTITUTTET

MILJØ – RESSURS – HAVBRUK

Nordnesparken 2, Postboks 1870, 5817 Bergen

Tlf.: 55 23 85 00 Fax: 55 23 85 31

Forskningstasjonen

Flødevigen

4817 His

Tlf.: 37 05 90 00

Fax: 37 05 90 91

Austevoll

Havbruksstasjon

5392 Storebø

Tlf.: 56 18 03 42

Fax: 56 18 03 98

Matre

Havbruksstasjon

5198 Matredal

Tlf.: 56 36 60 40

Fax: 56 36 61 43

Distribusjon:

OPEN

HI-prosjektnr.:

10.17.01

Oppdragsgiver(e):

DeepSpill JIP

Oppdragsgivers referanse:

Cortis Cooper, Chevron
Petroleum Technology Co.

Rapport:

FISKEN OG HAVET

NR. 14 - 2001

Tittel:

Potential implications on the pelagic fish and zooplankton community of artificially induced deep-water releases of oil and gas during DeepSpill_2000 --- an innovative acoustic approach

Senter:

Center of Marine
Environment

Seksjon:

Marine- and Experimental
biology, Physical
Oceanography

Forfatter(e):

Tor Knutsen and Bjørn Serigstad

Antall sider, vedlegg inkl.:

37

Dato:

15.12.2001

Sammendrag – norsk :

I forbindelse med DeepSpill_2000 (Johansen et al., 2001) ble det gjennomført flere utslipp av olje og gass fra 844 meters dyp på Helland-Hansen feltet i Norskehavet. I forkant av og i forbindelse med disse utslippene ble det benyttet et variert sett av prøvetakingsutstyr, ekkolodd og annen instrumentering for å overvåke og dokumentere miljøforhold, olje og gassutslipp samt biologisk aktivitet i området. Hovedmålet med undersøkelsene var å beskrive de biologiske ressursene og deres variabilitet i eksperimentperioden og dessuten skaffe seg informasjon om den akustiske tilbakespredningen fra organismer i vannsøylen. Ved å studere den akustiske tilbakespredningen fra organismene som utgjør det dype ekkolaget (DSL) og samtidig undersøke tilbakespredningen fra oljen og gassen som ble sluppet ut, var det mulig å få ny innsikt i interaksjonen mellom dyptlevende biologiske ressurser og oppadstigende olje/gass.

Ved bruk av ekkolodd kunne olje og gass lett observeres under alle utslippsforsøkene, og en del utvalgte situasjoner er presentert i rapporten. Den akustiske tilbakespredningen fra det dype ekkolaget mellom 300-500 m og dets naturlige variabilitet er dokumentert. Det er vist at oppadstigende olje/gas influerer de ellers ganske homogene DSL strukturene, selv om mekanismene for hvordan dette skjer ikke er avdekket enda. Når all tilbakespredning som med sikkerhet kunne tilskrives olje/gass ble ekskludert, var den gjenværende akustiske tilbakespredning fra det dype ekkolaget nesten en størrelsesorden høyere enn det en finner når en sammenligner med en upåvirket situasjon. Årsakene til dette er enda ikke tilstrekkelig klarlagt, men noen hypoteser er skissert i rapporten. At en fraksjon av oljen eller kanskje særlig gassen som ble sluppet ut, av ulike årsaker har en forlenget oppholdstid i dybdeområdet som omfattes av det dype ekkolaget (DSL), kan være den mest nærliggende forklaring på dette fenomenet.

Sammendrag – engelsk :

During the DeepSpill_2000 field experiment (Johansen et al., 2001) oil and gas were artificially released on several occasions from a water depth of 844 meters at the Helland-Hansen site in the Norwegian sea. Prior to and during these releases a variety of sampling gear, echo sounders and other instrumentation were used to monitor and obtain information on the environmental conditions, oil and gas plumes and the biological activity in the experimental region. The main objective of the present work has been to provide a general description of the biological community of the experimental region, and to provide information on the variability of biological scatterers throughout the water column. By exploring and evaluating the short-term variability of the biological scattering structures, the organisms therein and concurrently examine scattering from the released oil and gas, new insights on how rising oil and gas might interact with the deep-water plankton and fish community of the experimental region could be gained.

Acoustic scattering from oil and gas was easily observed during all experimental spill events and some situations are presented in this report. The magnitude of the acoustic scattering from organisms inhabiting the Deep Scattering Layer (DSL) between 300-500 m depth for an undisturbed situation and its natural variability is documented. It is shown that rising oil-gas plumes certainly influences the otherwise quite homogeneous DSL structure, although the precise mechanisms involved are still not revealed. When all scattering, from structures that with certainty can be attributed to the released oil and gas were excluded, the remaining acoustic scattering from the DSL seem to be nearly an order of magnitude higher compared to an undisturbed situation. The reason for this is still uncertain, but some tentative hypotheses are formulated. The most plausible explanation seem to be that a fraction of the released compounds and in particular gas bubbles, for various reasons have a prolonged residence time within the region of the DSL, hence contributing significantly to the increased scattering observed during the spills.

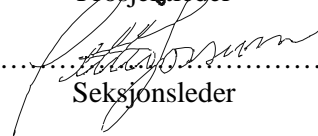
Emneord - norsk:

1. Biologiske ressurser
2. Utblåsning
3. Akustikk

Emneord - engelsk:

1. Biological resources
2. Blowouts
3. Acoustics


.....
Prosjektleder


.....
Seksjonsleder

Potential implications on the pelagic fish and zooplankton
community of artificially induced deep-water releases of
oil and gas during DeepSpill_2000 --- an innovative
acoustic approach

by

Tor Knutsen and Bjørn Serigstad

Institute of Marine Research (IMR)

Center of marine Environment

Nordnesgaten 50, P.O. Box 1870 Nordnes

N-5817 Bergen,

Norway

Content

1 Introduction	3
2 Materials and Methods	3
2.1 Meteorology	3
2.2 Current measurements	4
2.3 Hydrography	4
2.4 Acoustic measurements	5
2.5 Biological sampling	5
2.6 Topography of the study area	6
3 Results and analyses	7
3.1 Hydrography	7
3.2 Current measurements	8
3.3 Biology	10
3.3.1 <i>Abundance and vertical distribution of mesozooplankton and krill</i>	10
3.3.2 <i>Distribution and abundance of fish, squid and macrozooplankton</i>	13
3.4 Acoustic scattering structures	15
3.5 Fish and zooplankton distribution in relation to scattering structures	17
3.6 Acoustic scattering structures during the diesel and methane release	19
3.7 Acoustic scattering structures during the crude oil and methane release	22
3.8 Acoustic scattering structures during the final methane and seawater release	23
3.9 Increased scattering within DSL	25
4 Conclusions	26
5 Suggestions for future work	27
6 References	29
7 Acknowledgements	31
Appendix I Mesozooplankton as obtained with Mocness	32
Appendix II Mesozooplankton as obtained with Multinet	35
Appendix III Mesozooplankton as obtained with the WP II net on 29 June 2000	36
Appendix IV Overview of samples collected for chemical and biomarker response analyses	37

1 Introduction

Prior to and during the DeepSpill_2000 field experiment on the artificial release of oil and gas at the Helland-Hansen site (22 June – 1 July 2000) (Johansen et al., 2001), a sampling program was undertaken using a variety of sampling gears, echo sounders and other instrumentation in order to collect information on the environmental conditions and the biological activity in the experimental region.

In general, the short period the organisms were exposed to oil/gas contaminants during the experimental releases, and the restricted magnitude of these spills, suggested that it might be difficult to trace and document through chemical analyses any biological contaminants effecting animal populations in the deepwater habitat. By sub-sampling the biological samples obtained with the various nets and trawls, some groups of organisms were selected for analysis of oil components and biomarker responses. The target organism was the copepod *Calanus finmarchicus* or “raudåte” which is probably the most important zooplankton in the Norwegian Sea during summer (Wiborg, 1954; Østvedt, 1955, 1965; Hirsche, 1994). These samples will however await further analysis until expressed interest from participating parties should indicate otherwise.

Hence, the main objective of this study was to produce a general description of the distribution and abundance of organisms inhabiting the water masses in the region, and to provide quantitative data on the vertical distribution of living organisms, which in turn can be used to improve bio-impact models. Secondly, it should provide information on the variability of biological scatterers throughout the water column, as observed and quantified by the echo sounders. Such variability or changes in distribution pattern can result from natural processes like diurnal vertical migration of organisms, horizontal migration, patch formations or schooling behavior of plankton and fish (c.f. Simard et al., 1986; Simard and Mackas, 1989; Melle et al., 1993; Kaartvedt et al., 1996; Torgersen et al., 1997). It is envisaged that some organisms might actively avoid the artificial releases and the adjacent region if they have the necessary swimming capacity. On the other hand, horizontal flow, as well as displacement of organisms caused by physical forcing induced by the released compounds should also be considered. Given these constraints an approach was chosen, namely exploring and evaluating the short-term variability of the biological scattering structures, the organisms therein and how these might relate to observed scattering from the released oil and gas.

2 Materials and Methods

2.1 Meteorology

Relevant meteorological information on wind speed, wind direction, sea state, cloud cover was obtained from the weather stations onboard RV Johan Hjørt and RV Håkon Mosby. However, no measurements of light irradiance and light attenuation in the water column were performed from any of the participating vessels. As light conditions are important for the vertical migration and distribution of organisms in the water column (Kaartvedt et al., 1996), the lack of such measurements is a deficiency, but not critical. The light summer nights at high latitudes as during the current deep spill experiments at 65°N, implies that the changes in light conditions between night and day are only moderate. In order to have some information on the general light regime in the

Helland-Hansen region during field experiments that is relevant for the biological activity, a table giving the computed times for sunrise and sunset in the region have been produced (Table 1). From this table it is seen that the summer “night” is actually of very short duration or more precisely about 2 hours in mid June.

Table 1. Sunset and sunrise at 65⁰N, 04⁰50'E [GMT+ 1 hour] according to tables computed by the U.S. Naval Observatory. To obtain Norwegian summer time 1 hour should be added to the given times.

June 2000		
Date	Sunrise	Sunset
19	0142	2343
20	0141	2343
21	0142	2343
22	0142	2343
23	0143	2343
24	0143	2342
25	0145	2341
26	0146	2340
27	0148	2339
28	0149	2337
29	0151	2335
30	0154	2333

2.2 Current measurements

On RV H. Mosby a RD Instruments 150 kHz narrowband hull mounted Acoustic Doppler Current Profiler (ADCP) was used to monitor the current pattern in the upper part of the water column from approximately 20 - 400 m depth. Raw and averaged data were stored in a computer onboard the research vessel and later processed at IMR with support from the Geophysical Institute, University of Bergen.

In order to perform near continuous measurements of current velocity in the deeper part of the water column, a RDI Long Ranger 75 kHz ADCP were mounted on a moored rig at a bottom depth of around 830 m. A LinkQuest Inc. acoustic modem (UWM 2000) were used to upload data in near real time, but data were also stored internally in the instrument for later post-processing by IMR/Sintef-Chemistry. The LR ADCP current measurements were performed for 25 m depth bins, ranging approximately 33.3 m to 508.3 m from the instrument, corresponding to an actual depth range of 800 – 320 m depth.

2.3 Hydrography

A Seabird 911 CTD with a water bottle rosette sampler was used to obtain information on the temperature and salinity conditions in all parts of the water column to approximately 20 m above the bottom and to obtain water samples at selected depths for chemical analysis of oil components. Both CTD-transects and individual and irregular CTD stations were taken. From RV Johan Hjort a total of 23 CTD-stations were performed during the experimental period. From RV H. Mosby only two CTD-stations (or casts) were obtained and the water bottle rosette sampler was not used.

2.4 Acoustic measurements

On RV Johan Hjort continuous acoustic measurements were performed using the Simrad EK500 scientific echosounder connected to 18, 38, 120 and 200 kHz transducers. All transducers were mounted on a retractable keel (Ona and Traynor, 1990) in order to obtain high quality data, during potentially severe weather conditions. The Bergen Echo Integrator (BEI) was used to store all acoustic data in a database, as well as for inspection of the acquired data during the cruise (c.f. Foote et al., 1991). With respect to the 18 and 38 kHz transducers, data were acquired with a range setting of 0-750 m or 0-1000 m, while the 120 and 200 kHz transducers were operated with a range setting of 0-250 m.

On board H. Mosby the EK500 and BEI system was used as on RV Johan Hjort. Data were however, mainly acquired at 38 kHz during the oil spills, using an identical range setting as on RV Johan Hjort. A limited amount of recordings were also made at 120 kHz.

2.5 Biological sampling

The biological sampling program was undertaken from RV Johan Hjort, when time allowed. Depth stratified mesozooplankton sampling was performed with a 180 µm meshed Multiple Opening and Closing Net Environmental Sampling System (MOCNESS) (Wiebe et al., 1976; 1985) towed obliquely at 2 knots. Sampling depths for the MOCNESS were from 700-500 m, 500-400 m, 400-300 m, 300-200 m, 200-100 m, 100-50 m, 50-25 m and 25-0 m. A 180 µm meshed Multinet having five separate nets (Anon., 1990), was additionally used in a similar way, but operated vertically rather than being towed as the MOCNESS. Sampling depths for the Multinet were 800-700 m, 700-500 m, 500-300 m, 300-100 m and 100-0 m.

To obtain information on the fish and macrozooplankton community (mainly krill and mesopelagic shrimps), a pelagic Harstad trawl was used, trawling for approximately 30 minutes at four different depths; 690, 500 and 250 m depth, completing the series with the larger Åkra-trawl in the surface region (0-30 m), using floats attached to the trawl. The Harstad trawl and Åkra trawl cannot be closed or opened by remote commands. Hence, they will sample fish and macrozooplankton both on their way down the water column to the predetermined sampling depth, and on its way back to the surface. However, the trawling time at sampling depth is long compared to the time used at any other depth, hence contamination of the samples by organisms being mainly distributed in other parts of the water column are assumed to be small. Stratified sampling at different depths as during the present study, also help to identify which species are sampled outside the main sampling depths. In order for the trawl samples to be compared with respect to catch abundance all numbers have been normalised to a trawling distance of 1 nautical mile.

An additional sampling series also targeting mesozooplankton, particularly the copepod *Calanus finmarchicus* or “raudåte”, was performed using a single 180 µm meshed WP II net (Anon., 1968). These were integrated samples from the upper part of the water column, either from 200-0 m or 100 m to the surface. The samples were mainly conducted to obtain biological material for later chemical analysis of oil components and biomarker response measurements, and were stored in a freezer at -20°C or in liquid N_2 .

The samples obtained with MOCNESS, Multinet and WP II nets were treated and worked up according to standard IMR procedures for mesozooplankton sampling. Data on species composition is given in Appendix I-III. First, each sample was usually divided in two parts, one for biomass estimation and the other for species identification and enumeration. The biomass part was size fractionated using sieves of 2000 μm , 1000 μm and 180 μm mesh size, hence giving biomass size fractions $>2000 \mu\text{m}$, $>1000 \mu\text{m}$ and $< 2000 \mu\text{m}$, and $>180 \mu\text{m}$ and $< 1000 \mu\text{m}$. The biomass samples for each size fraction were placed on pre-weighed aluminum dishes and put in an oven at $60 \text{ }^{\circ}\text{C}$ for approximately 20 hours onboard the research vessel. Upon drying the samples were stored in a freezer at $-20 \text{ }^{\circ}\text{C}$ for the remaining part of the cruise. On returning to IMR they were further dried in a laboratory oven at $60 \text{ }^{\circ}\text{C}$ for 3 hours. The samples for species identification were stored on 100 ml flasks and fixated to a 4 % formalin and seawater solution for later species identification in the laboratory at IMR. In addition fish, krill and shrimps were removed from the biomass size fraction $>2000 \mu\text{m}$, counted, weighed and lengths measured.

An overview of the samples collected for chemical analyses and biomarker response measurements are given in Appendix IV.

2.6 Topography of the study area

The DeepSpill_2000 experimental locality was situated in a small region at the Helland-Hansen site with the discharge point at 65°N , $04^{\circ}50'\text{E}$ and 844 m depth. This region is situated south of the Vøring Plateau on the continental slope between the Norwegian Sea deep water to the west and the more shallow continental shelf region to the east (Figure 1).

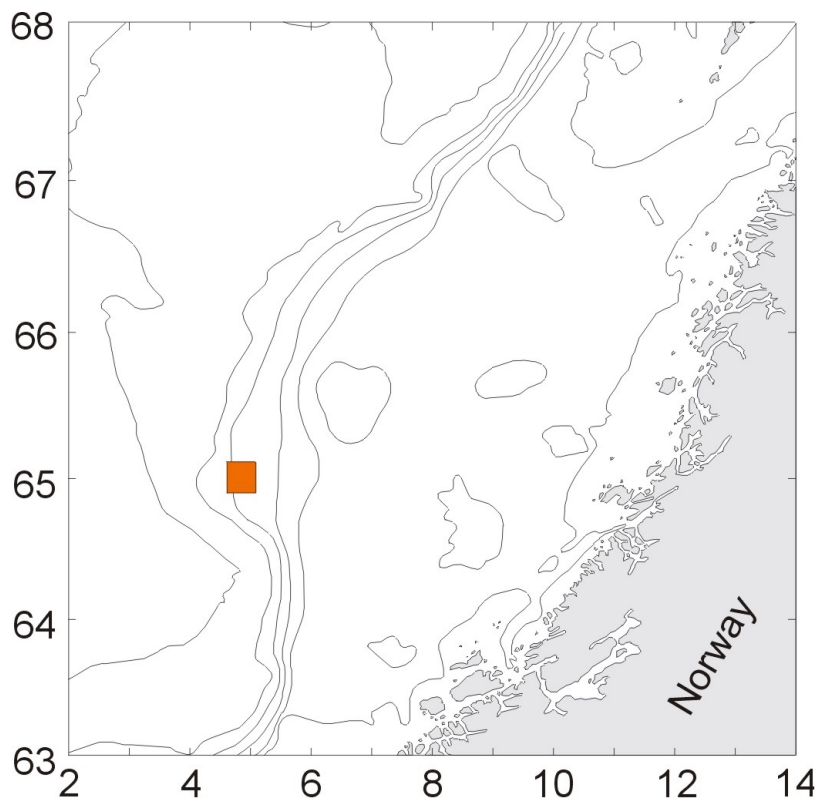


Figure 1. The DeepSpill_2000 experimental region (red square) with surrounding bottom topography.

In this continental slope region bottom topography is usually changing rapidly towards increasing depths when moving from east to west (see Figure 1), and bottom contours are running parallel in an overall northerly direction. However, the horizontal extension of the experimental region was quite restricted and the bottom depth showed only slight changes within the region. It is to be expected that bottom topography is important for the general current pattern in this region and that topographic steering of the current will be important, not least in the few hundred meters above the bottom.

3 Results and analyses

3.1 Hydrography

A hydrographic transect running from west to east consisting of six ctd-stations (St 480 - St 485) was obtained on 23-24 June 2000, slightly north-east of the discharge point at $65^{\circ}N$, $04^{\circ}50'E$ (Figure 2). The horizontal extension of this transect was about 15.7 km, but due to problems with the data processing, St 480 has not been included in the presentation of the temperature and salinity data as seen in Figure 2. It is obvious that within this restricted area, rather homogeneous and well-defined water masses are found.

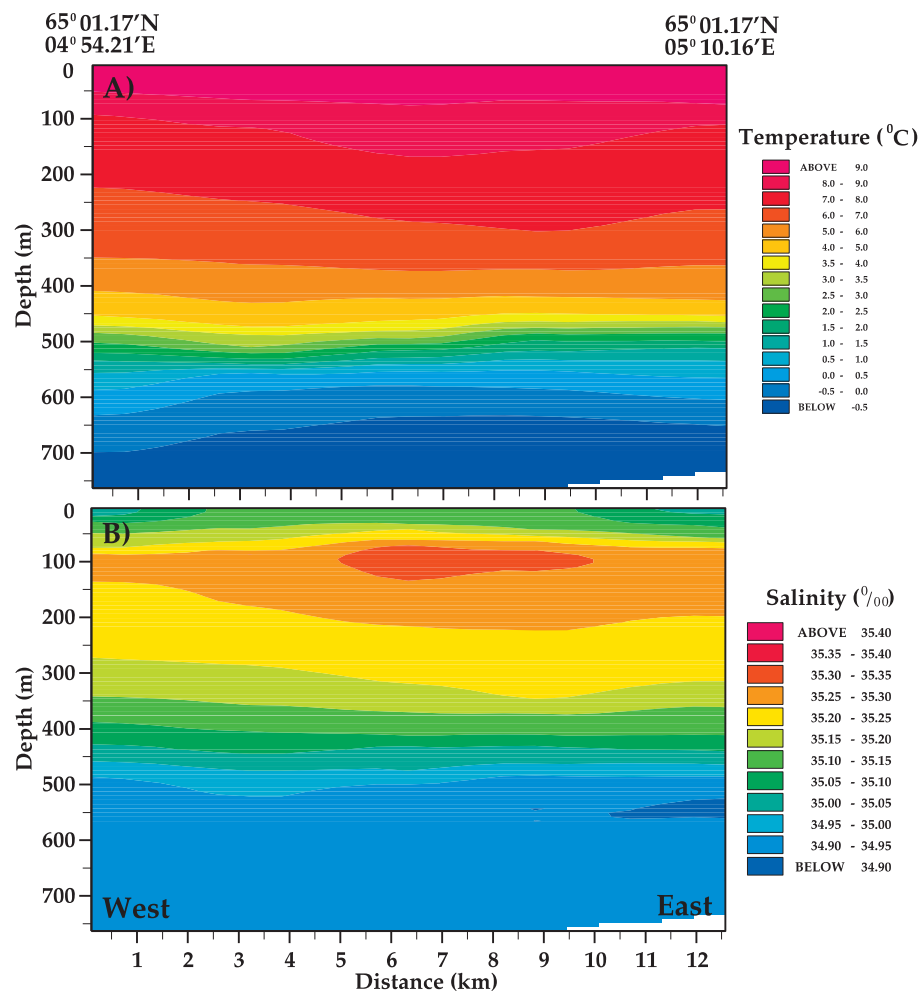


Figure 2.
CTD transect
showing the
salinity and
temperature
distribution
on 23-24 June
2000.

In Figure 3 is given the vertical distribution of temperature and salinity at St 481 which is the westernmost station on the transect as shown in Figure 2. Between the surface waters and 400 m depth a warm ($>5^{\circ}\text{C}$) and saline ($>35^{\circ}/_{\text{oo}}$) water mass occur, by definition called Atlantic Water due to its salinity and temperature characteristics. Below 500 m depth Norwegian Sea Deep Water (NSDW) is found, being particularly evident from the salinity profile (Figure 2),

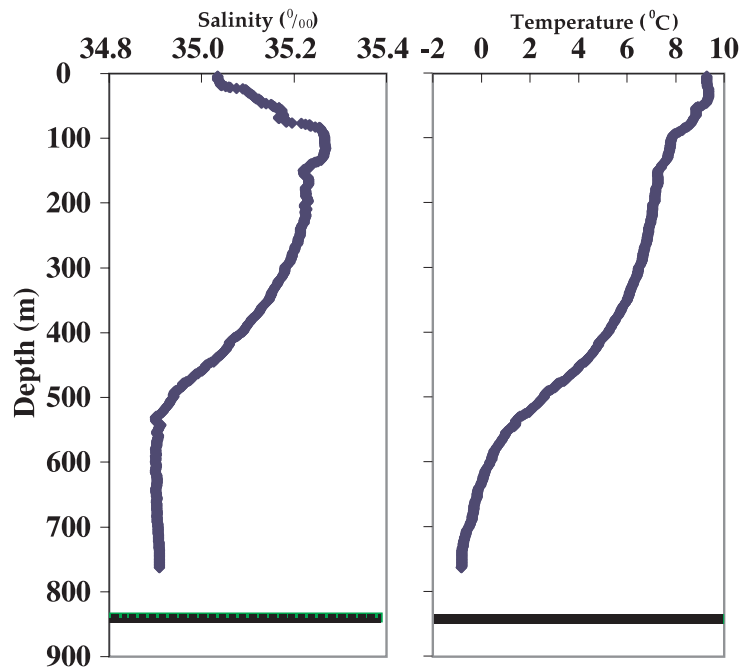


Figure 3. Vertical distribution of temperature and salinity at St 481 on 24 June 2000.

the salinity being close to $34.9^{\circ}/_{\text{oo}}$, while temperature decreases from around 2°C to about -0.8°C close to the bottom. A transition zone between Atlantic Water and Norwegian Sea Deep Water is found between 400 and 500 meter. The core of Atlantic Water seems to be found around 100-150 m depth, given the high salinity ($>35.2^{\circ}/_{\text{oo}}$) recorded in this region for a larger part of the transect. The less saline water found in the surface region compared to the core Atlantic Water residing around 100 m depth, suggests an influence of water from the shelf region to the east.

3.2 Current measurements

An overview of the current pattern for part of the water column is presented in Figure 4. It is seen that there was a more or less eastward transport of water in the uppermost part of the water column as observed from the bottom mounted ADCP at 325 m depth. This is well within the region of Atlantic Water as described in the previous chapter. In the transition region between Atlantic Water and the Norwegian Sea Deep Water, represented by the current measurements at 520 m depth, current direction is slightly more variable, and displacement of water is more restricted. At 750 m depth, approximately 100 m above the bottom, the current is quite stable with regard to direction but turning north north-west at about UTC 06:00 on 27 June. After this time the water displacement is actually significantly larger at this depth than what is observed at 325 m depth. The current direction at 750 m depth suggests as indicated

earlier that topographic steering is important, as the bottom contours are running in a north north-westerly direction in the experimental region (c.f. Figure 1).

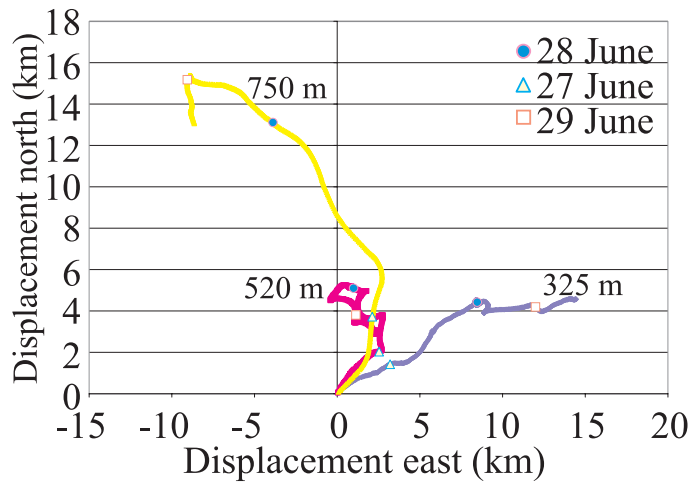


Figure 4. Current pattern as shown as a progressive vector diagram of the currents in 325 m, 520 m and 750 m depth through the period 26 June [UTC 14:36] to 29 June [UTC 13:26].

In Figure 5 is shown the current velocity at three different depths in the deeper part of the water column. Overall current velocities are moderate, only exceeding 10 cm/s for small periods of time. The semidiurnal tidal influences on the current velocity are apparent, particularly on the east-west velocity components.

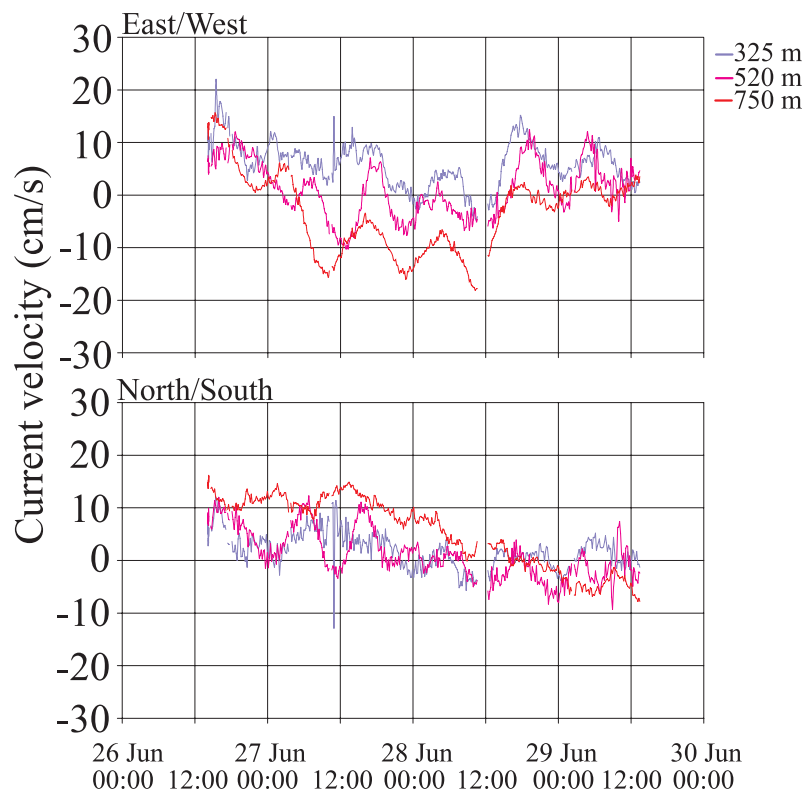


Figure 5. Current velocity (cm/s) at 325 m, 520 m and 750 m depth through the period 26 June [UTC 14:07] to 29 June [UTC 13:26]. Velocity east and south are negative. Data based on 10 minute averaged bins from the bottom mounted ADCP.

Within the observation range of the bottom mounted ADCP, the current velocities were usually highest in the deepest part of the water column. At an intermediate observation range (~ 520 m) current velocities were slightly lower but with the current frequently changing direction (Fig. 5). Around 325 m again increased current velocities were recorded, but with a reasonable stable direction towards north-east (Fig. 4 and 5).

The current pattern in the upper 400 m of the water column was measured using the ship mounted ADCP on RV Håkon Mosby. Due to the bin averaging interval being 10 minutes, the original averaged ADCP data contained a lot of spikes or “bad quality” data due to frequent change of ship heading and speed. Although it might be possible to improve these data set by redoing the averaging of the raw ADCP data, that is applying a shorter averaging interval, this option has not been considered during the first phase of the project due to time constraints. Instead synthetic time series of the currents in the upper part of the water column have been constructed (see Johansen et al., 2001). These are based on the bottom mounted ADCP data from 348 m depth and some good quality measurements for quite restricted time periods obtained with the ship mounted ADCP as references (Johansen et al., 2001). Hence, the ship mounted ADCP data have not been evaluated in the present report.

3.3 Biology

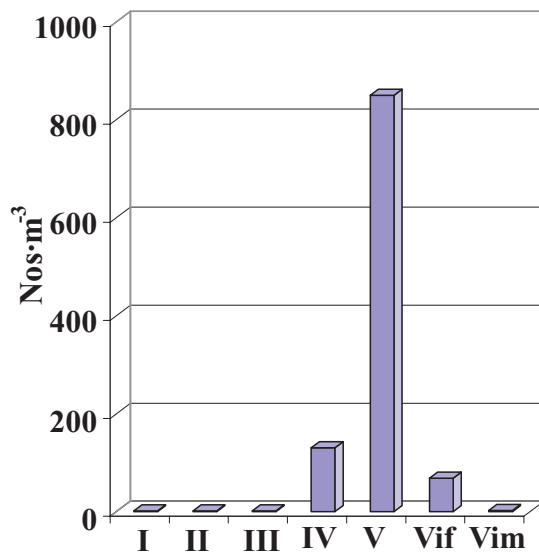
A total of three MOCNESS sampling series were conducted. An overview of the these data are given in Appendix I. The first two series prior to the DeepSpill_2000 experiment, on 24 June at 13:35-14:39 UTC and 16:42-18:08 UTC, while the third was conducted in the evening of 29 June at 17:09-18:21 UTC. With respect to Norwegian summer time, the MOCNESS sampling were completed in the early afternoon and in the evening approximately 8, 4.5 and 4 hours prior to sunset at the respective dates. Due to malfunctioning of the MOCNESS opening and closing mechanism during the first tow, no samples were obtained for the depth intervals 50-25 m and 25-0 m. The vertical distribution of mesozooplankton biomass were measured using both the MOCNESS and Multinet samplers. The presented results are however those obtained with the MOCNESS. The zooplankton species data obtained with the Multinet and WP II net are however for completeness given in Appendix II and III respectively.

3.3.1 Abundance and vertical distribution of mesozooplankton and krill

Of mesozooplankton dominating in the MOCNESS samples the copepod *Calanus finmarchicus* was by far the most important organism with regard to species abundance. No other organisms whether copepods or other types of mesozooplankton can compare. In Figure 6 is given the stage composition as the average number of *Calanus finmarchicus*, in the upper 50 m of the water column based on the second MOCNESS tow on 24 June 2000. Since diurnal vertical migration is probably not an important part of *C. finmarchicus* behaviour (Melle and Serigstad 2001) these data are taken as representative for the experimental region during mid summer.

Stage CV, usually considered as the main overwintering stage, completely dominated the population at this time of the year with a maximum in abundance in the 25 – 0 m depth interval of approximately 1400 ind. m⁻³.

Also other stages were recorded, but were much less numerous than CV. Stage CIV and adult females (CVIf) were found, but these only accounted for 12.4% and 6.5% of the total number of *Calanus finmarchicus* in the upper 50 m of the water column. Only in the 700 – 500 m depth interval a slight increase in the abundance of *C. finmarchicus* were recorded ($\sim 125 \text{ ind. m}^{-3}$), compared to depths between 50 and 500 m but still only about 7.5 % of what was found in the upper 50 m of the water column. Also in the very

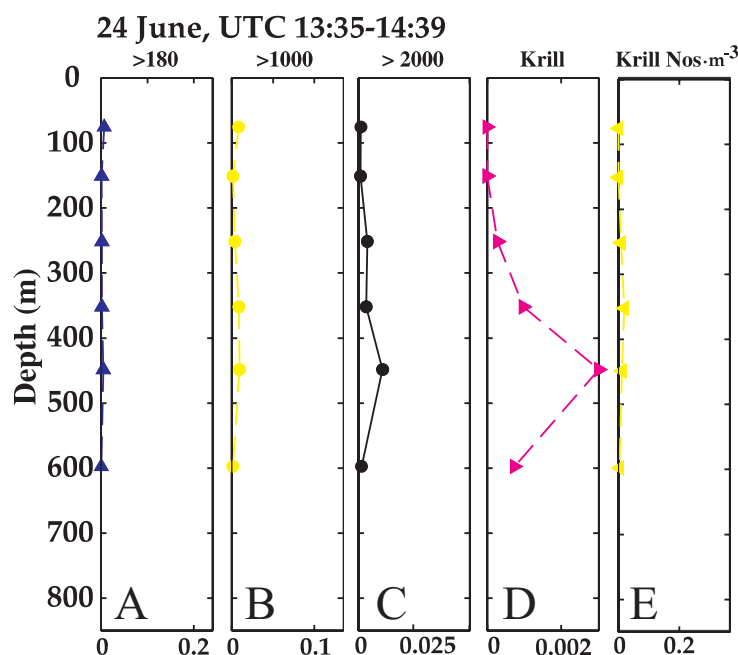


deepest part of the water column stage CV dominated, accounting for approximately 96.6% of total number of *C. finmarchicus* found. Stage CIV being the predecessor to CV showed an average abundance of about 14 % of the total *C. finmarchicus* population between 50 and 400 m depth.

Other copepods or mesozooplankton taxa were only recorded in very small numbers throughout the water column, the exception being *Oithona* spp. that showed a peak in abundance ($\sim 650 \text{ ind. m}^{-3}$) in the 50 – 25 m depth interval.

Figure 6. Mean number of individuals (Nos m^{-3}) of *Calanus finmarchicus* stage CI-CVI on 24 June 2000, 16:42-18:08 UTC in the depth interval 50 – 0 m.

Mesozooplankton and krill biomass (g m^{-3}), during the first MOCNESS tow on 24 June is shown in Figure 7. A peak in biomass was recorded in the deeper part of the water column between 300 and 600 m, particularly for the size fraction $>2000 \mu\text{m}$ and also for the euphausiids or krill. The maximum krill biomass ($\sim 0.02 \text{ g m}^{-3}$) and the low



number of euphausiids per m^{-3} suggests larger individuals, as was also confirmed by length measurements of the animals, these being around 24-27 mm in total length.

Figure 7. Mesozooplankton size fractionated biomass (g m^{-3}), krill biomass (g m^{-3}) and krill Nos m^{-3} as obtained with the MOCNESS on 24 June 2000 at UTC 13:35-14:39. Size fraction $>180 \mu\text{m}$ and $<1000 \mu\text{m}$. B) Size fraction $>1000 \mu\text{m}$ and $<2000 \mu\text{m}$. C) Size fraction $>2000 \mu\text{m}$. D) Krill biomass and E) krill numbers.

The krill being confirmed as the species *Meganyctiphanes norvegica*, residing at its daytime depth. No krill was found at depths less than 100 m. In the deeper part of the water column the size fraction $>2000 \mu\text{m}$ was dominated by larger carnivorous zooplankton organisms like chaetognaths (*Sagitta* spp.), the jellyfish *Aglanta digitale* and the copepod *Euchaeta* spp. The size fractions $>180 \mu\text{m}$ and $>1000 \mu\text{m}$ are often termed the *Calanus*-fraction because when abundant, this species usually dominates these two size fractions. Of these, the coarsest size fraction $>1000 \mu\text{m}$ are usually dominated by stages CVI (adult males and females), CV and CIV. Although it is evident that a significant proportion of the CIV's might be forced through the sieve at $1000 \mu\text{m}$, hence also contributing to the biomass as measured for the size fraction $>180 \mu\text{m}$, this size fraction usually is dominated by *C. finmarchicus* stages CI, CII and CIII. In order to evaluate the biomass data in the upper 50 m of the water column, that could not be obtained during the first MOCNESS tow, the second sampling series obtained three hours later then the first tow and approximately 4.5 hours prior to sunset are presented in Figure 8.

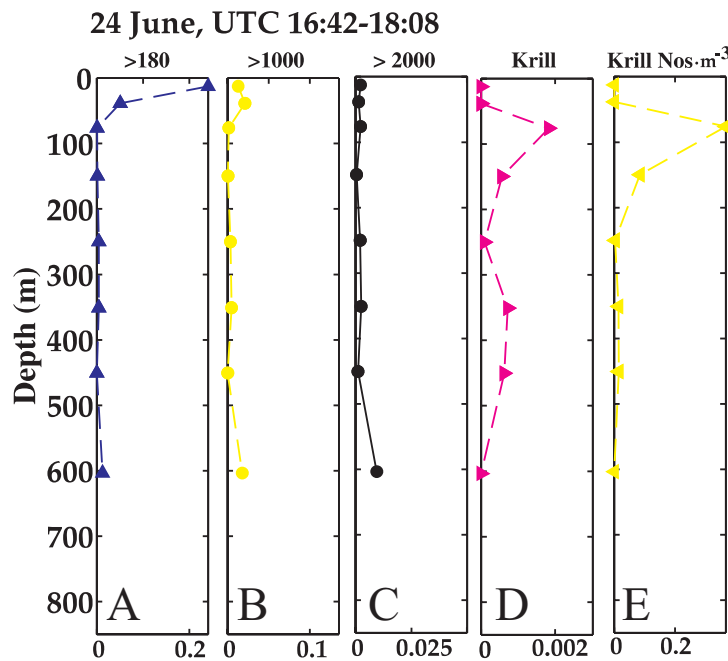


Figure 8. Mesozooplankton size fractionated biomass (g m^{-3}), krill biomass (g m^{-3}) and krill numbers as obtained with the MOCNESS on 24 June 2000 at UTC 16:42-18:08. A) Size fraction $>180 \mu\text{m}$ and $<1000 \mu\text{m}$. B) Size fraction $>1000 \mu\text{m}$ and $<2000 \mu\text{m}$. C) Size fraction $>2000 \mu\text{m}$. D) Krill biomass and E) krill numbers.

From the second tow on 24 June 2000 we observe that there is a significant increase in zooplankton biomass in the upper 50 – 0 m of the water column and that actually the biomass for the $>180 \mu\text{m}$ size fraction accounts for approximately 94% of the size fractionated biomass amounting to 0.24 g m^{-3} . Again krill biomass shows higher values between 300 and 500 m depth and another peak at about 75 m depth. The peak in abundance at 75 m depth reflects a corresponding peak in the krill numbers. The species data shows that the krill responsible for this peak is solely due to *Thysanoessa longicaudata*, a seasonal migrant that is confined to the uppermost waters in the Norwegian Sea during summer. At a mean depth of 150 m there is a mixture of two species dominated by smaller individuals of *M. norvegica*, mean total length 15.9 mm and *T. longicaudata* having a mean length of 12 mm. The species found deeper than 200 m were mainly larger (and older) individuals of *M. norvegica* with a mean length of 32 mm and a few individuals of *Nematoscelis megalops*, a species often found in smaller numbers in deep waters of Atlantic origin along the Norwegian coast.

On 29 June the third MOCNESS sampling was conducted. Results are in accordance with earlier tows (Figure 9). High biomass values are found in the upper 50 – 0 m of the water column for the $>180 \mu\text{m}$, $>1000 \mu\text{m}$ but also the $>2000 \mu\text{m}$ fraction now shows higher biomass values than the tow conducted 5 days earlier. Again two peaks in krill distribution are observed both with respect to biomass and to number of ind. m^{-3} . However, the uppermost krill peak now seem to be situated closer to the surface at a mean depth of 35.5 m, while the deeper maximum is located to a mean depth of approximately 300 m. Again, the uppermost peak is solely due to *T. longicaudata*, although this species is also found in low numbers throughout the water column down to approximately 500 m depth.

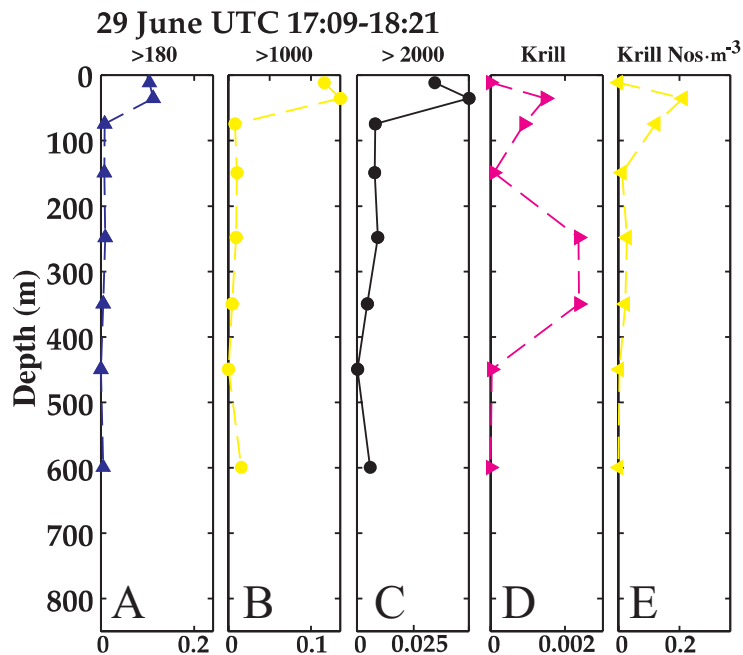


Figure 9. Mesozooplankton size fractionated biomass (g m^{-3}), krill biomass (g m^{-3}) and krill Nos m^{-3} as obtained with the MOCNESS on 29 June 2000 at UTC 17:09-18:21.

A) Size fraction $>180 \mu\text{m}$ and $<1000 \mu\text{m}$. B) Size fraction $>1000 \mu\text{m}$ and $<2000 \mu\text{m}$. C) Size fraction $>2000 \mu\text{m}$. D) Krill biomass and E) krill numbers.

At a mean depth of 75 m again a mixture of *M. norvegica* (68.2%) and *T. longicaudata* (31.8%) are found. The krill biomass peak in the deeper part of the water column (Figure 8), is mainly due to larger individuals of *M. norvegica* (mean length 27.2 mm), although a comparable number of small *T. longicaudata* was found as well.

When the situation as observed with the MOCNESS on 24 June is compared to that on 29 June we realize that particularly the krill component seem to be located at slightly shallower depths (see Figure 8 and 9). The tow on 29 June was conducted somewhat later in the evening, only about 4 hours prior to sunset, which is also slightly earlier on 29 June compared to 24 June (see Table 1). Hence the change in euphausiid distribution is most likely a result of these animals migrating towards the surface layers when surface irradiance decreases, favoring an upward migration.

3.3.2 Distribution and abundance of fish, squid and macrozooplankton

Organisms like fish, shrimps, squid and large krill are usually not sampled quantitatively by the mesozooplankton sampling gear (i.e. MOCNESS, Multinet and WP II nets), although the MOCNESS is giving reasonable estimates on the occurrence of small krill, while it certainly underestimates the large krill. In order to obtain more information on the occurrence of these larger sized components of the biological

community, a series of depth stratified hauls were performed using the Harstad trawl (Godø et al., 1993), while the Åkra trawl (Valdemarsen and Misund, 1995), was used to sample the uppermost 30 – 0 m of the water column. In Table 2 are given the results of the pelagic trawl samples.

Table 2. Numbers (N) and wet weight biomass (W) in grams of fish, macrozooplankton and squid per 1 nautical mile trawled distance. Time is duration of trawl at sampling depth. - : No counts available.

Depth (m)	N		W		N		W		N		W		N		W		N		W	
	690-675		490-500		287-250		30-0		480-500		270-250		30-0		480-500		270-250		30-0	
Date	24-06-2000		24-06-2000		24-06-2000		24-06-2000		27-06-2000		28-06-2000		29-06-2000		27-06-2000		28-06-2000		29-06-2000	
Time (UTC)	0510	0538	0738	0809	1030	1100	1208	1237	1931	2005	1341	1411	1549	1618	1931	2005	1341	1411	1549	1618
	Early morning		Morning		Mid day		Mid day		Evening		Afternoon		Early evening							
White barracudina [Notolepis rissoi kroyeri]	2.6	39.3	0.7	11.0					1.3	8.4										
Blue whiting [Micromesistius poutassou]	6.1	345.0	4.4	402.9	2.6	137.3			1.9	118.2	0.9	28.4								
Lantherne fish [Benthoema glaciale]	14.0	15.7	38.1	54.9	36.6	13.7			10.4	13.6	4.7	2.8								
Hatchet fish [Argyrolepeceus spp.]	1.7	0.9																		
Haddock 0-group			0.7	4.4	0.7	3.9	138.4	703.9											3.5	13.1
Herring larvae					0.7	0.3													2.1	0.7
Herring							0.6	205.4												
Mackerel							0.6	241.7											0.7	280.9
Lumpsucker							0.6	39.3											0.7	57.4
Saithe							1.2	1.2												
Isopoda	0.9	4.4																		
Pasiphea spp. (shrimp)	3.5	12.2	2.9	6.2	1.3	0.7			10.4	27.3										
Sergestes arcticus (shrimp)	7.0	8.7	63.7	42.5					27.9	37.0	7.6	24.6								
Hymenodora sp. (shrimp)	20.1	32.3	13.9	16.1	-	1.3														
Meganyctiphanes norvegica [krill]	528.4	111.5	368.5	103.3	78.2	20.3			7.1	1.5	11.4	1.9								
Thysanoessa longicaudata [krill]			136.9	6.5	60.4	2.9														
Thysanopoda acutifrons [krill]	1.7	5.2																		
Other smaller zooplankton	-	189.5	-	6.5	-	48.9			-	27.9	-	48.3								
Periphylla sp.	1.7	668.1			0.7	32.7					0.9	300.5								
Other jellyfish					3.3	228.8		-	4410.9											
Gonatius fabricii (squid)										1.3	23.4								0.7	0.7

Particularly to be noted is the composition and abundance of some major groups of organisms in the deep pelagic hauls obtained at depths deeper than about 450 m. At these depths the white barracudina, blue whiting and the lantern fish seem to be the dominating fish species. Another important group of organisms is the mesopelagic shrimps *Pasiphea* spp., *Sergestes arcticus* and *Hymenodora* sp., which is numerous both in numbers and biomass at these depths. Krill or euphausiids is the third group of organisms that is a prominent member of the deepwater pelagic community at these depths, as could also be noted from the Mocness samples (see Figure 6).

At mid day there are also traces of the same groups of organisms in more shallow waters, around 250-300 m depth. However the deepwater shrimps are less numerous, while euphausiids is still caught in fair numbers (Table 2). It is noted that the size distribution of the dominating euphausiid *M. norvegica* (Figure 10) shows predominantly larger individuals (30-40 mm total length) in the deepest part of the sampled water column while at more intermediate depths only individuals around 25 mm total length are caught. Overall this is in accordance with the results from the Mocness tows, although it is important to realize that largest euphausiids probably avoid the Mocness sampling gear due to their high swimming capacity.

It must also be kept in mind that during pelagic trawling organisms are collected both on its way up and down the water column. Hence larger catches in the deeper hauls might also reflect a substantially longer trawling time and a greater volume sampled than what would be the case for more shallow hauls.

In the upper 30 – 0 m of the water column a very different community exist. In this region of the water column adult herring, mackerel and lumpsucker were found, but not in very high numbers. Also herring larvae were observed along with 0-group haddock which were caught in high numbers in one of the surface hauls. However, also in the deeper hauls 0-group haddock were found although they were probably caught in the near surface layers upon return of the trawl or during its deployment.

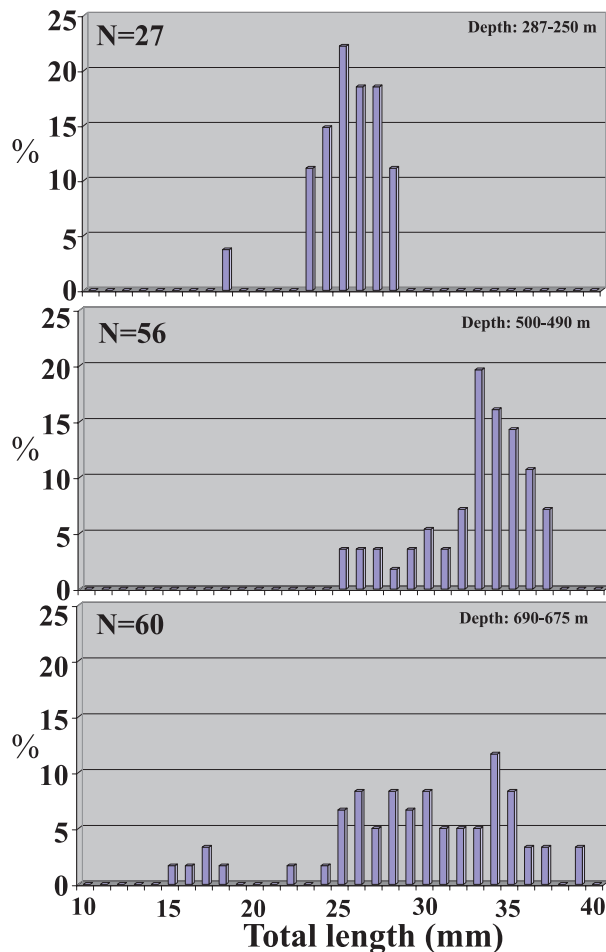


Figure 10. Size distribution of the euphausiid *M. norvegica* during three consecutive hauls in the deeper part of the water column on 24 June 2000.

3.4 Acoustic scattering structures

The acoustic scattering structures as observed with the echosounder at 38 kHz are usually regular and continuous in appearance, at least within a few nautical miles (Fig. 11). Some variability in the magnitude of the acoustic scattering structures are however found to be present, mostly due to increased abundance of organisms in particular regions or due to local patchiness of fish or zooplankton. A typical daytime and nighttime echogram is shown in Figure 11 as recorded on 28 June. The daytime echogram is typical of the registrations to be expected in the study region during summer. A Deep Scattering Layer (DSL) is found between 250 – 500 m depth. The area backscattering coefficient (s_A), later for convenience termed “acoustic density”), recorded over a 1 nautical mile distance amount to around 400 – 2000 m^2/nm^2 (Fig. 11) or sometimes slightly higher. What can be seen here is not uncommon and is solely attributed to the abundance of animals within this depth range, changing slightly in abundance through the recording period. It can be particularly noted that upper part of this DSL is composed of stronger scatterers confined to small patch like structures. During daytime another more weak but distinct scattering structure was observed above the main DSL, between 200 – 300 m depth, with acoustic density in the range 7 – 12

m^2/nm^2 . A characteristic feature during daytime is the shallow scattering structure (SSL) extending from approximately 15 to near 50 m depth.

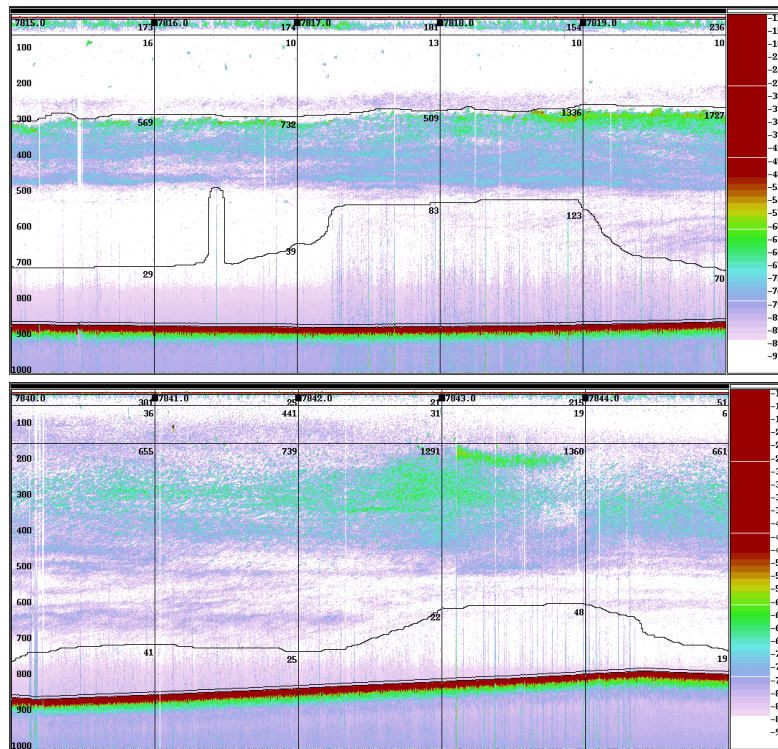


Figure 11. Echogram from the EK500 at 38 kHz during daytime 28 June [UTC 09:10-10:20] (upper panel) and during night [UTC 21:50-01:36] (lower panel). Color scale shows volume backscattering strength (S_v) in dB.

This SSL is similar in appearance to the upper part of the DSL and it is envisaged that an important component of both structures are small fish, although the fish species are certainly not the same. At night the scattering structures change significantly in appearance (Fig. 11). Compared to the daytime DSL which is centered around 400 m depth, the DSL during night is less defined with highest backscattering values at around 300 m depth. Due to the reduced light irradiance during night many of the organisms found in the daytime DSL have probably ascended to more shallow waters. However, the total backscattering observed during night below approximately 200 m depth, is of the same order of magnitude as that observed during day (Fig. 11). During night there is also a significant increase in the scattering observed between 100 – 200 m depth, resembling what was observed between 200 – 300 m during daytime hours. Another characteristic feature, at least for the record shown in Figure 11, is the absence of the shallow scattering structure (SSL) that was observed during day down to approximately 50 m depth. This suggests that the organisms originally responsible for the main scattering here, actually move to even shallower depths during night.

It can also be remarked that there seems to be slightly higher scattering below 500 m depth during night compared to the insignificant daytime scattering at this depths. This might be due to organisms that at daytime reside closer to the bottom, now vertically migrates in sufficient numbers into a region where they are detected by the 38 kHz echosounder.

In Figure 12 is shown the acoustic backscattering integrated over a horizontal distance of 0.1 nautical mile during a 24-hour period on 23-24 June 2000. At this frequency the organisms responsible for the backscattering observed are mainly fish and macro-zooplankton like large shrimps and euphausiids if sufficiently abundant to be detected at depth. The figure particularly illustrates aspects of the regular diurnal vertical migration of the fish and macro-zooplankton inhabiting the slope waters of the Norwegian Sea during mid summer. Even at this time of the year a substantial part of the biomass that is located below 300 m depth during daytime, ascend into the

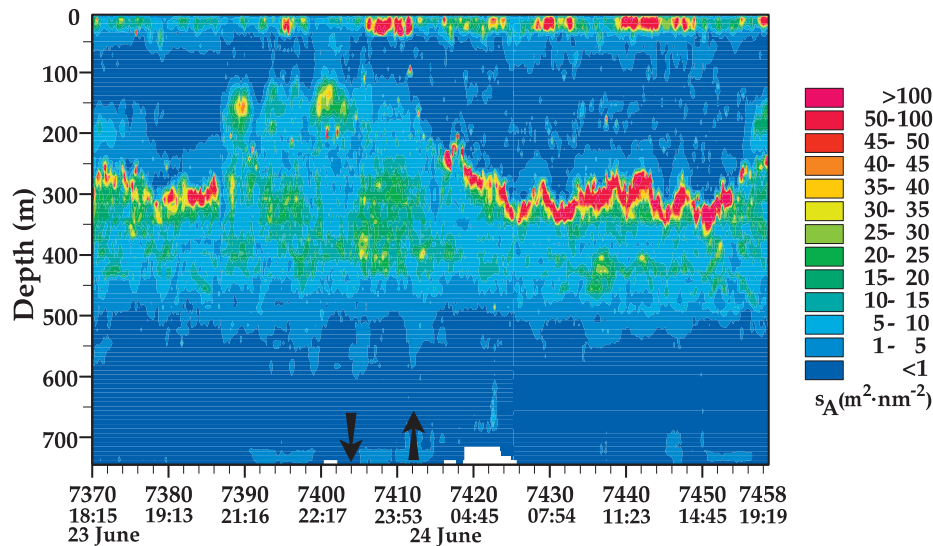


Figure 12. Acoustic scattering structures during a period of approximately 24 hours showing diurnal vertical migration of fish and macrozooplankton as reflected in the area backscattering coefficient (s_A) at 38 kHz. Arrows indicate times of sunset (down) and sunrise (up) respectively. Both time of day in UTC and sailed distance is given along x-axis.

uppermost 200 m and even shallower waters during night. However, care must be taken in interpretation as it is evident that there must also be high abundance of particular groups of organisms below 500 m depth, which due to inherent characteristics of echosounder at 38 kHz are not usually detected at these observation ranges. That is, smaller organisms like krill and mesopelagic shrimps, which according to the trawl data are apparently numerous also below 500 m depth.

3.5 Fish and zooplankton distribution in relation to scattering structures

From our sampling using the Mocness and the pelagic trawls, as well as previous experience (Melle et al., 1993; Kaartvedt et al., 1996; Torgersen et al., 1997), the daytime DSL observed between 300 and 525 m is most certainly composed of mesopelagic fishes such as the lantern fish (*Benthosema glaciale*), blue whiting (*Micromesistius poutassou*), white barracudina (*Notolepis rissoi kroyeri*), hatchet fish (*Argyrolepecus* spp.), mesopelagic shrimps like *Sergestes arcticus*, *Pasiphea* spp., *Hymenodora* sp., although it is more or less unknown how these groups of organisms are located within this vertically extended DSL as shown in Figure 11. Within the DSL a substantial amount of euphausiids or krill are also located, particularly *Meganyctiphanes norvegica*. However, from the Mocness and pelagic trawl data (Figure 7-9 and Table 2) it is evident that euphausiids are abundant both deeper in the

water column and at more shallow depths, although their abundance at particular depths will strongly depend on their vertical diurnal migration.

The weak scattering structure observed between 200-300 m during daytime (Figure 11), has an appearance suggesting the presence of euphausiids. In Figure 13 is given the acoustic registrations as recorded during the Mocness tow on 24 June, along with the krill biomass and abundance recorded during the same tow. The scattering structures are quite similar to those shown in Figure 11, but with slightly stronger scattering in the upper 100 m.

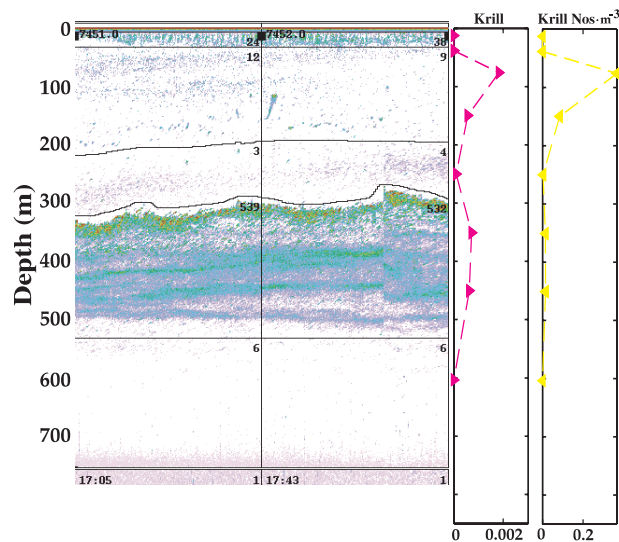


Figure 13. Echogram obtained at 38 kHz during the Mocness tow conducted on 24 June [UTC 16:42-18:08]. The echogram covers the time period UTC 17:07-18:52. Color scale as Figure 11.

Both from Figure 13 and 14 there seem to be a reasonable agreement between the weak scattering structures observed around 300 m depth and the krill biomass and abundance found at this depth. Correspondingly the increased scattering observed between approximately 50 and 100 m, seem to coincide with increased krill abundance at these depths.

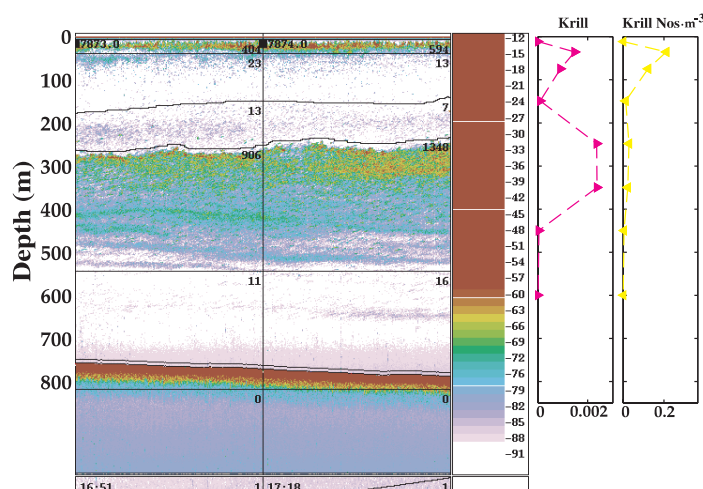


Figure 14. Echogram obtained at 38 kHz during the Mocness tow conducted on 29 June [UTC 16:42-18:08]. The echogram covers the time period UTC 16:51-17:49.

In the surface scattering layer also denoted SSL (>15 m and <50 m depth) certainly the fish is the most significant scattering component. The only smaller scatterer documented to be present in large numbers is *Calanus finmarchicus* (c.f. Figure 6-9), but which at least theoretically should not contribute significantly to the acoustic backscattering at 38 kHz. The trawl catches (c.f. Table 2), show the occurrence of

0-group haddock, some 0-group and adult herring, the squid *Gonatus fabricii*, some mackerel and lumpsucker, and these are probably the organisms responsible for the patchy acoustic backscattering recorded in the near surface region at 38 kHz.

3.6 Acoustic scattering structures during the diesel and methane release

During the diesel and methane release on 27 June, the Deep Scattering Layer (DSL) seems to change markedly compared to what was observed prior to the release on 24 June (Fig. 13) and to an “undisturbed” situation as recorded on 28 June (c.f. Fig. 11). In Figure 15 are shown a high-resolution compressed image of the acoustic data obtained at 38 kHz from RV Johan Hjort.

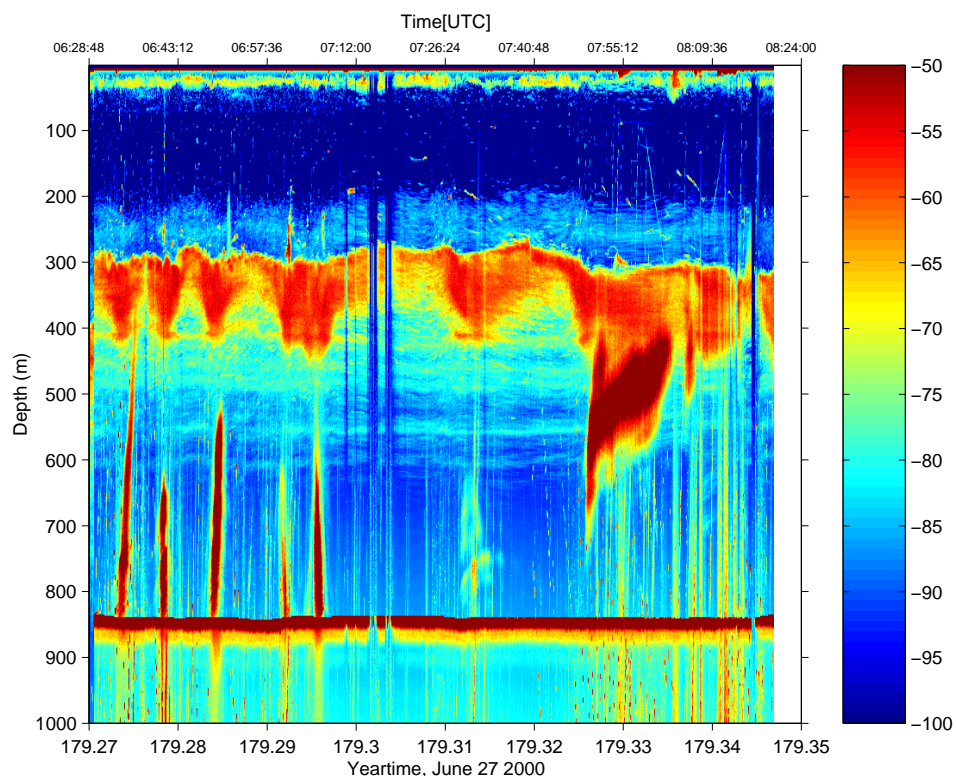


Figure 15. Acoustic scattering structures during the diesel-methane release on 27 June [UTC 06:29-08:19] as recorded from RV Johan Hjort. Color scale shows volume backscattering strength (Sv) in dB.

This figure is plotted with time as x-axis rather than distance-time as for the log-based echograms presented elsewhere, in order to present the rapid changing events in the time domain only. Figure 16 shows a log-based echogram for part of the same period obtained from RV H. Mosby. Interestingly, from both research vessels similar acoustic scattering patterns emerge. Using the Deep Scattering (DSL) layer [between 300 and 500 m depth] as a reference, we realize that this layer shows an apparent “wave”-like pattern, with repetitive dome shaped formations. The acoustic backscattering intensity changes in a near sinusoidal manner, at least within the first 1 ½ hours of the spill. The diesel/methane “plume” is rising abruptly from the bottom region as 100 % pumping rate of these compounds is achieved at approximately 08:37 local time [UTC 06:37] (Johansen et al., 2001). Although there is not always an exact match between the rising diesel and gas, and the localization of the dome shaped formations as seen from the

echograms, we suggest that there is a close connection between these two apparent observations. It is realized that the current pattern shows quite different overall directions at different depths (c.f. Figure 4-5). Hence, it is no surprise that a dome shaped structure might be detected a bit off-axis with respect to a rising gas and oil plume. The dome shaped formations results from cyclical changes in the backscattering intensity, being weaker at some point and stronger at others. In fact this seems to be quite different from undisturbed recordings of the same DSL, which are much more regular and homogeneous in appearance (c.f. Fig. 11 and 13). It must be noted that these changes are found in the lower region of the DSL, facing the rising plume. On some occasions, in the topmost region of the DSL situated at approximately 300 m depth, there seems to be signs of the scattering structures being “lifted” or forced to slightly shallower depths, see Figure 15.

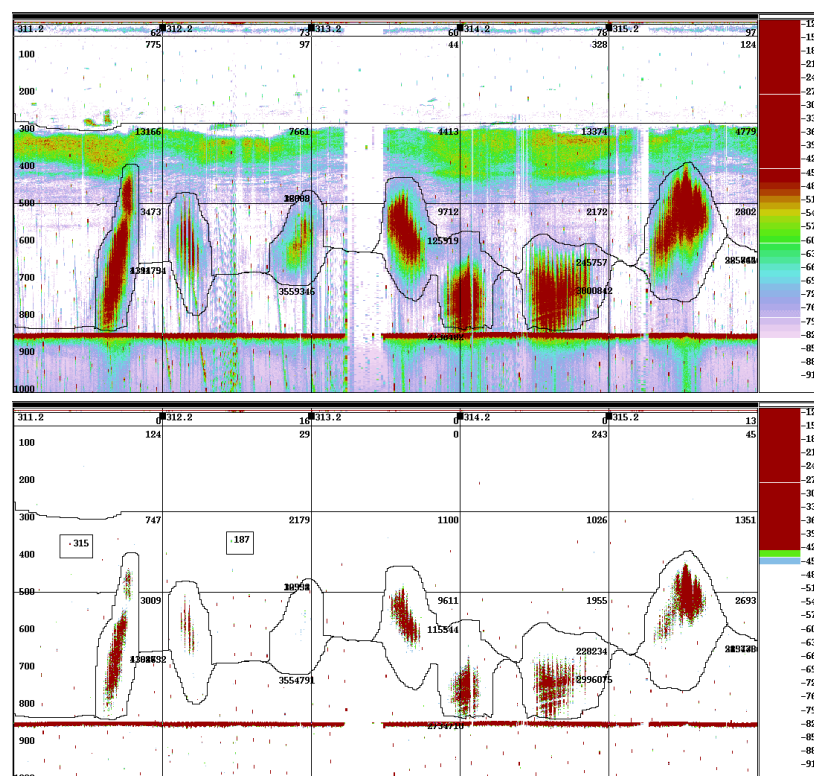


Figure 16. Acoustic recordings at 38 kHz obtained from RV H. Mosby on 27 June [UTC 06:57-07:27]. Upper panel showing dome shaped structures and most of the smaller scatterers included, with volume backscattering strength (S_v) down to -82 dB. Lines surrounding the diesel/methane structures are used to delineate these from other scattering structures. Lower panel illustrates thresholding excluding S_v -values below -45 dB, leaving the acoustic recordings of the methane/diesel and ADCP-noise stand out. Within the DSL as delineated by the layer lines at 300 and 500 m the area backscattering coefficient is given for comparison as the numbers in the upper right hand corner of each rectangular region. Two smaller rectangular boxes also called “schools” show acoustic contribution of a single “red-spot” (transmit pulse) ADCP noise.

Even if all scattering caused by the diesel-methane release are subtracted as attempted and visualized in Figure 16, the remaining scattering confined to the DSL structure, is substantially higher than what was observed prior to the experimental spill (c.f. Fig. 13) as well as for an “undisturbed” situation (Fig. 11). During the first phase of diesel/methane spill on 27 June, s_A values recorded over a 1 nautical mile distance in the DSL (300-500 m depth) amount to 10000 – 15000 m^2/nm^2 [RV Johan Hjort, Log 7761- 7764, not shown]. This is in the order of 8-10 times the values recorded [400 – 2000 m^2/nm^2] for a more “natural” situation (Fig. 11). It should be remarked that immediately prior to the diesel/methane release seawater and nitrogen were released for approximately 30 and 45 minutes respectively in a more or less continuous operation (Johansen et al., 2001).

We realize that the two nautical miles of sailed distance that has the highest area backscattering values within the DSL are Log 311.2: 13166 m^2/nm^2 and Log 314.2: 13374 m^2/nm^2 . Applying a threshold of –45 dB, remove “weaker” scattering structures in the range –45 to –82 dB. This allows the acoustic recordings of the methane/diesel release and the ADCP noise stand out, and to roughly determine the contribution of the ADCP-noise within the DSL. In these two cases the ADCP noise was determined to 1062 m^2/nm^2 and 1026 m^2/nm^2 respectively, meaning that only 7-8 % of the area backscattering values could be attributed to this type of noise.

The key question as to the origin of the dome shaped structures within the DSL, is how they might have been generated. A set of hypotheses is suggested;

The sinusoidal structure observed could be an internal wave passing or one that has been generated by the energy in the rising diesel and methane “plume”. However, a passing internal wave is less plausible as these usually are “disturbances” that travel along pycnoclines and the water masses between 300 and 400 m are quite homogeneous where the domes are located (c.f. Fig. 2 and 3). Also there is no evidence that a cyclical pattern was present for the undisturbed recordings obtained prior to or after the releases. It is also doubtful if the energy in the rising methane/and diesel is sufficient to generate an internal wave. The reasonably close coupling between the rising diesel/methane structure and the dome shaped formations might favor other explanations.

The dome shaped structures could also be formed by animals moving away from a region subject to diesel and gas as most marine organisms avoid such regions if they have the swimming capacity to do so, although attraction to oil polluted regions have also been documented (Serigstad et al., 1997). On the other hand there are events or recordings where the diesel/gas “cloud” seem to be surrounded by the DSL without any apparent dome visible (RV H. Mosby, Log 317.2, not shown) which might contradict the previous suggestion. However, this event was observed 1 hour after the start of the diesel/gas release, hence the character and dynamics of the “cloud” at this point in time might have changed considerably compared to what was observed during the initial phase of the spill.

Another plausible scenario is that the ascending “plume” is powerful enough to enforce water to be displaced vertically generating a water front that contains significantly less organisms than the average values found within the DSL. Hence a dome shaped structure might be generated, that from an acoustic point of view shows significantly less scattering within the dome compared to the surrounding region. Such a process might have been initiated by the seawater/nitrogen release and then strengthened by the methane/diesel release that immediately followed.

3.7 Acoustic scattering structures during the crude oil and methane release

During the crude oil and methane release on 29 June there are few if any signs of the dome shaped structures as was clearly evident during the diesel and methane release conducted on 27 June. This holds for the acoustic backscattering as observed both from RV H. Mosby and RV Johan Hjort. However, the backscattering values recorded within the Deep Scattering Layer (DSL) are also during this spill quite high compared to values recorded for an “undisturbed” situation. Why there is no apparent dome shaped structures present during this spill is not easy to explain. It might be due to several factors. Replacing diesel with crude oil, might significantly have altered the dynamics of the spill, hence the rising crude oil/gas “plume” is less defined and influences its surroundings in a different manner compared to the combined diesel/gas release. It should be remarked that the duration of the nitrogen and seawater release prior to the crude oil/gas spill were approximately identical to the equivalent nitrogen/seawater release preceding the diesel/gas spill on 27 June.

Even if no dome shaped structures were observed during the crude oil/methane release, there are some inhomogeneity in the acoustic recordings within the DSL that seem to be associated with the crude oil/methane release. This can be seen both from the RV Johan Hjort and RV H. Mosby recordings (Fig. 17). However, explanations as to the mechanisms behind their formation will at this point be purely speculative.

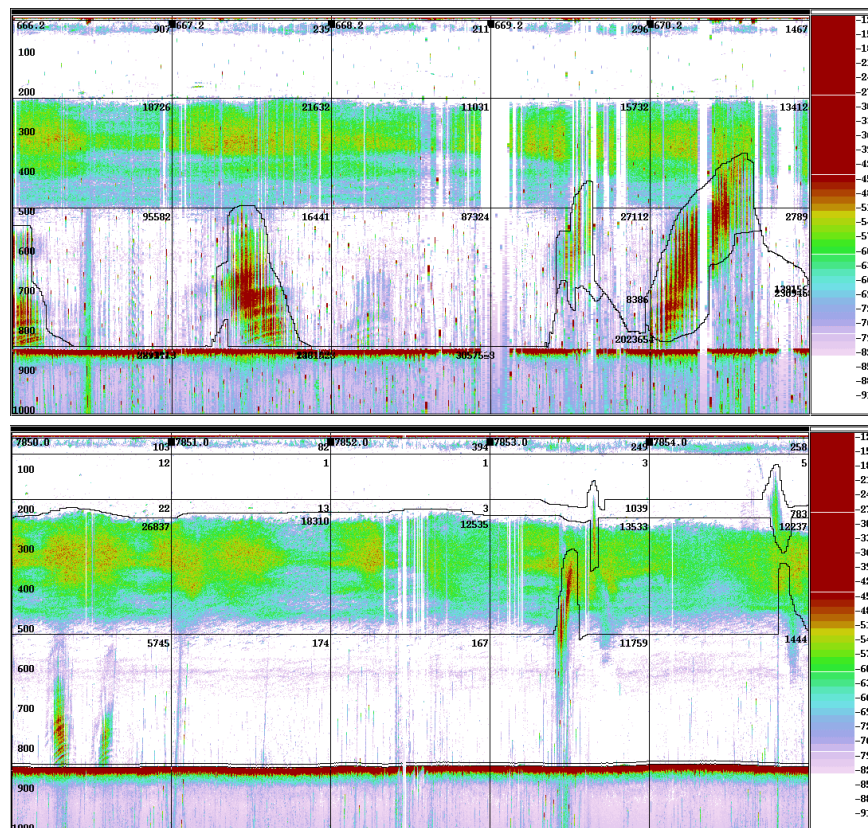


Figure 17. Acoustic recordings at 38 kHz obtained during part of the crude oil/methane release on 29 June 2000. Upper panel from RV H. Mosby [UTC 05:24-05:54] and lower panel RV Johan Hjort [UTC 04:28-06:59].

Also during this spill the backscattering recorded within the DSL shows significantly higher values, 11000-19000 m^2/nm^2 (RV H. Mosby) and 12000-27000 m^2/nm^2 (RV Johan Hjort), than what has been recorded for an “undisturbed” situation as exemplified through Figure 11. It is worth noting that the integrator values are near identical for the two ships, again suggesting that the ADCP-noise recorded from RV H. Mosby is not significantly biasing the total backscattering within the DSL.

3.8 Acoustic scattering structures during the final methane and seawater release

The final release on 29 June was performed with methane and seawater only. This spill event lasting approximately 2-2 ½ hours was only observed through the echosounder on board RV H. Mosby. Also during this spill no apparent dome-shaped structures was observed. The seawater and methane released during this spill was observed easily on several occasions or passes, from the bottom region to approximately 400 m depth, coinciding with the lowermost region of the DSL. Signs of small “cloud” like structures appear above the top of the DSL at around 250 m depth and about 40 minutes after the start of the spill (Figure 18). Other structures slightly different in appearance to the first two structures occur above 250 m depth, about 57 minutes after the start of the spill and again 6 minutes later (Fig. 18). These last two structures are certainly not of biological origin and must be due to either the seawater or methane released during the spill or both

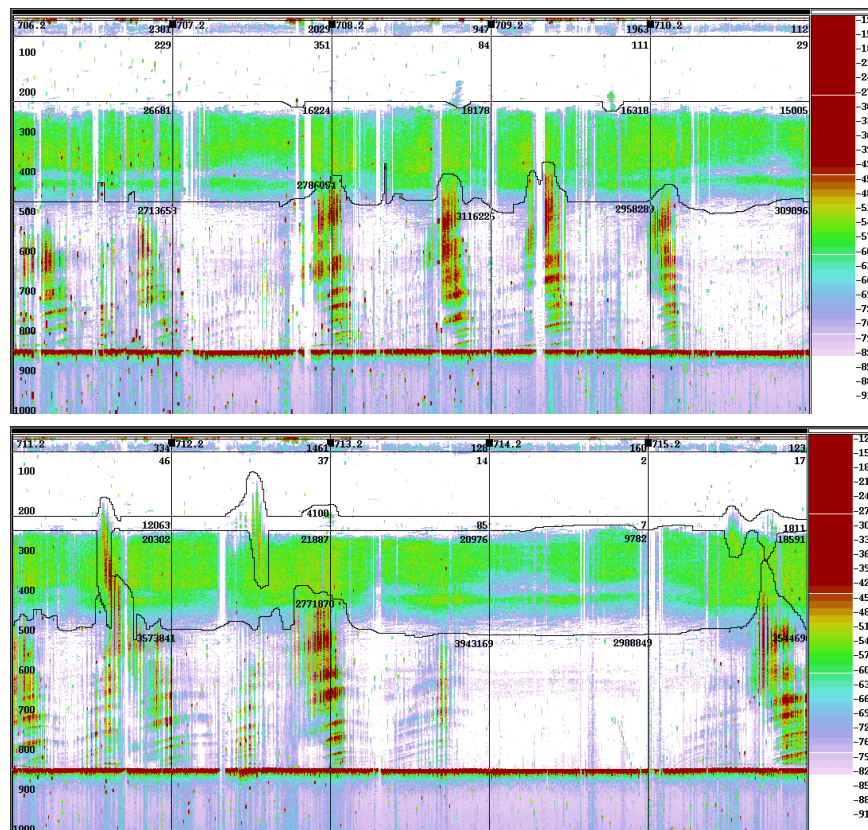


Figure 18. Acoustic scattering structures as obtained at 38 kHz from RV H. Mosby during part of the seawater/methane release on 29 June. Upper panel UTC 09:54-10:24. Lower panel UTC 10:24-10:54. Vertical lines denote 1 nautical miles sailed distance.

compounds together. The last two recordings can also be seen clearly within the DSL. As for the previous spills it is evident that the acoustic backscattering values within the DSL are significantly higher than what can be accounted for by organisms and ADCP-noise alone. In the presented figure it has not been attempted to exclude this noise in an extensive manner, only to delineate the DSL from the methane/seawater recordings below approximately 450 m and from the recordings in the upper 200 m of the water column. It is quite apparent that within the few hundred meters of the DSL region, the backscattering caused by the methane/seawater release significantly change in appearance, become weaker and is nearly absent above the DSL. It can be speculated that in addition to the pure physics involved when seawater is mixed with adjacent water at depth, and gas bubbles of various sizes rise towards the surface, there is also a biological barrier to be crossed by the released compounds. This is particularly true for the methane, as the released seawater is probably completely mixed with the surrounding water within 100-200 m above the bottom (Ø. Johansen, pers. comm.). The acoustic recordings of the methane/seawater spill is easily seen up to 400 m depth, and on some occasions even shallower, suggesting that the transition zone between Atlantic Water and Norwegian Sea Deep Water as found between 400 and 500 meter is no definite barrier in a physical sense. Within the DSL, both salinity and temperature are reasonably homogeneous (c.f. Fig. 2 and 3). Hence there seems to be no sound reason why the gas should not proceed more or less uninterrupted through this region, which at least partly seems to be the case, as some methane is evidently detected above the DSL.

In order to show where the increased backscattering within the DSL is located with respect to the discharge point, and reveal the situation also beyond this region, the backscattering within the DSL is presented in Figure 19.

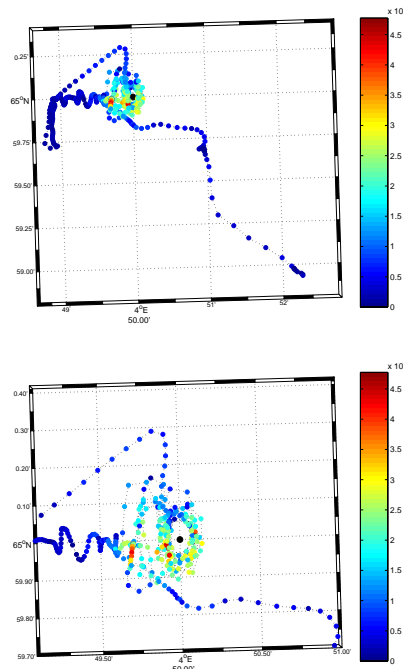


Figure 19. Integrated acoustic backscattering (s_A) in m^2/nm^2 at 38 kHz for the Deep Scattering Layer (DSL) as situated between 300 – 500 m depth during the methane/seawater release on 29 June 2000, until the echosounder was switched off [UTC 08:54-14:53]. Upper panel grand overview of the complete time period. Lower panel restricted view. All prominent ADCP-noise as well as all seawater/methane recordings that certainly can be assigned to the methane/seawater released during the experiment has been removed.

In this presentation all prominent ADCP-noise and all scattering that with certainty was assigned to the methane/seawater component as presented in Johansen et al. (2001) now has been excluded.

Figure 19 quite clearly suggests that the acoustic backscattering within the DSL significantly decrease as the ship move away from the central discharge region. The maximum recorded s_A -value amounts to $47746 \text{ m}^2/\text{nm}^2$, which admittedly suggests that some ADCP-noise is still present in the data. However, this presentation is more of a suggestive nature regarding further data exploration and analysis. Nevertheless it seems to support the idea that a significant higher scattering within the DSL is closely coupled to the discharge region although all scattering that were assigned to the methane/seawater release has in fact been subtracted.

3.9 Increased scattering within DSL

During all three spill events (diesel/methane June 27, crude oil/methane 29 June and methan/seawater 29 June), a very high backscattering was recorded within the DSL in connection with the release events despite that scattering structures earlier identified as caused by the oil and gas components have been removed. This is certainly difficult to explain based on our current limited knowledge on the abundance, distribution and behavior of biological scatterers within the DSL compared to an “undisturbed” situation. However, some tentative explanations regarding these results are suggested in the following;

- 1) naturally occurring higher density patches of macrozooplankton and mesopelagic fish was present in the monitored region during the spill.
- 2) organisms within the DSL could have been artificially attracted to the spill site from the surrounding region due the permanent position of Far Grip and the subsurface coil steel tubing structure found throughout the water column. Whether this could be an active process that involve organisms gathering in the vicinity of the coil steel tubing or a passive process, only involving organisms being displaced with currents is difficult to assess. Since the echosounder at the depth of the DSL mainly detect fish at a frequency of 38 kHz, it might be suggested that a possible aggregation of organisms are mainly caused by fish actively seeking the spill site region due to unknown cues. Here, turbulence and/or acoustic “noise” generated by rising oil and gas bubbles and/or the coil steel tubing could be the most relevant suggestion.
- 3) Another aspect affecting the magnitude of acoustic scattering is the tilt angle of the biological scatterers. If the tilt angle distribution of significant scattering organisms, due to unknown cues change, and more animals have a broadside incidence to the echosounder plane wave, a significantly higher scattering would be the result even if number of scatterers do not change.
- 4) rising oil droplets and/or gas bubbles might have been trapped or concentrated within the DSL, causing a significant increase in the acoustic backscattering observed. This could be due to a reduced ascent speed and distribution of particular

sized oil droplets and gas bubbles as they are physically brought in contact with, being captured or maybe adhere to organisms which are regarded as quite abundant within the DSL.

- 5) Various types of noise will always contribute at least to some degree to the scattering as monitored through an echosounder. In our case the transmit pulse generated by the hull mounted ADCP on board RV H. Mosby, which is not synchronized with the EK500 echosounder, is the most significant noise source. This type of noise is apparent on the RV H. Mosby echograms as scattered red spots, being especially prominent at depths below 400 m due to the Time Varied Gain (TVG). This type of noise was however not observed in the echosounder data from RV Johan Hjort during concurrent recordings, which also shows significantly increased backscattering values within the DSL. Most of the ADCP noise can however be removed easily by excluding from integration the most prominent “red spots” using the layer lines of the BEI post-processing system or by addressing these as “schools” using rectangular boxes for which the backscattering values can also be excluded (see Fig. 16). Hence, its contribution to the backscattering within the DSL is suggested to be less important.

We suggest that the idea of an active aggregation of animals within the DSL cannot explain the frequent very high backscattering values recorded in connection with the spills. Some aggregation of organisms and or a directional change in tilt angle of organisms cannot however be entirely ruled out, either as an active behavioral response to some unknown cues and/or passive aggregation with water masses. There is however no sign of an active ascent or descent of organisms within the DSL during the spills. What has been interpreted as a slight “lift” in the DSL coupled to the dome shaped structure observed during the first diesel/methane release, we suggest is only a passive process, organisms being slightly displaced vertically by the rising oil and gas plume. We suggest that the increased scattering within the DSL is mainly due to oil droplets and gas bubbles that for some reason have a prolonged residence time or are trapped within the DSL for some period of time. This might be caused by the high abundance of organisms that is evidently present in the DSL, suggesting that there is a higher probability of an increased encounter rate between organisms and oil droplets/gas bubbles in this region. Hence the concept of a biological barrier can be formulated, acting to reduce the ascent rate of the rising oil and gas. There seem to be no physical constraints regarding depth of release or water column temperature/salinity structure that could act to reduce the ascent speed of oil/gas in the observed a manner (c.f. Johansen et al., 2001). As the increased scattering seems to be equally high during the pure seawater/methane release on 29 June as for the other two releases involving also crude oil and diesel, it is suggested that the most significant contribution to the increased scattering is probably methane bubbles. Also from the seawater/methane release it can be seen that very few recordings of gas is observed shallower than 300 m depth, while significant recordings are found below 450 m depth. Hence, it seems that some important changes in the rising methane take place within the DSL.

4 Conclusions

Based on the results of this work as well as that presented in the main DeepSpill_2000 report (Johansen et al., 2001) we conclude that the acoustic methodology is a powerful technique in order to monitor spills and blow-outs of oil and gas at ocean depths of up

to 1 km. Simultaneously the abundance of many of the organisms inhabiting the same water masses, as well as aspects of their behavior and distribution can be monitored. These aspects along with traditional biological sampling and monitoring of deep water currents might be helpful in future like experiments, but can also provide valuable information following accidental blow-outs in order to better predict impact on environmental resources.

Some modeling exercises have shown that oil from a deep water blow out would be trapped in the water column, and that methane would form hydrates given the hydrographic conditions prevailing in the deep region of the Norwegian Continental slope (Rye and Johansen, 1999a,b). The findings presented in the present report and the results of the DeepSpill experiment with regard to the ascent dynamics of oil and gas (Johansen et al., 2001), should be further explored in order to understand how a fraction of the released compounds might contribute to the increased scattering observed within the DSL. As part of the modeling approach it is suggested that a sub-model should be included to take into account the presence of moving and drifting organisms as well as their abundance within particular regions of the water column.

A quite extensive treatment on the biological resources of the Norwegian Sea and a preliminary environmental risk analysis has recently been produced (Melle et al., 2001). Hence, such aspects have not been focused during the present study. It is evident from this as well as other studies that a substantial part of the biomass of macrozooplankton and fish resides in deep water region of the Norwegian Sea (Melle et al., 1993; Torgersen et al., 1997; Dalpadado et al., 1998). Therefore, from an impact perspective high priority should be given to address the potential coupling and mechanisms by which a Deep Scattering Layer (DSL) interact with a deep water spill of oil and gas.

With the present methodology and sampling frequency in space and time, partly violated by different interests with respect to research vessel operations, it is difficult to reveal direct links between the behavior and distribution of organisms and how they are effected by the rising oil and gas plumes. More elaborate *in situ* techniques should be applied to address such issues along with high resolution dedicated sampling of both organisms and chemical parameters.

When all scattering visually accepted as resulting from the oil and gas spills was removed from the acoustic data, there is still near an order of magnitude higher scattering within the Deep Scattering Layer (DSL) during the spill events compared to an undisturbed situation. This higher scattering cannot be accounted for by biological scatterers only. If it is caused by remnants of the oil and gas spills, it might at least have short-term effects on the biological community present in the experimental region, although the nature of such effects is partly unknown due to the great depth of these interactions (c.f. Melle et al., 2001).

5 Suggestions for future work

The results in the present report are still of a preliminary nature regarding the dynamics of the different spills, particularly on how an increased scattering can be possible in the region of the DSL. A more thorough analysis of these aspects than what has been possible in the present report is indeed of interest and should at some point be completed.

Acoustic modeling in a multi-frequency context could be used to assess oil droplet and gas bubble size distribution and abundance, hence their ascending velocity. Several potential recordings both in deep water and in the uppermost hundred meters when RV Johan Hjort is performing CTD casts, hence not moving, could be explored in this manner. The challenge of separating gas recordings from those of crude oil and diesel still remains intriguing.

Acoustic multi-frequency analysis could also be used in order to classify or discriminate between different biological structures as well as separating these from artificial recordings like the oil and gas structures evidently seen during this study.

The magnitude as well as frequency spectrum of the ambient “sound” environment should be monitored during future like experiments in order to understand how this differ from an “undisturbed” situation. By complementary use of under water cameras one could also address the question regarding tilt angle distribution of biological scatterers and its significance to increased scattering within the DSL.

6 References

- Anon., 1968. Smaller mesozooplankton. Report of Working Party No. 2. Pp. 153-159 in: Tranter, D.J. (ed.) *Zooplankton Sampling. (Monographs on oceanographic zooplankton methodology 2.)*. UNESCO, Paris. 174 pp.
- Anon., 1990. Instruction manual. Multiple plankton net A. Hydro-Bios, Post Box 8008,D-2300 Kiel 16, Germany.
- Anon., 2000. PAH probe, UV-Fluorometer for aromatic hydrocarbons. Manual version 1. Sea & Sun Technology GmbH, pp. 1-28.
- Dalpadado, P., Ellertsen,B., Melle,W. and Skjoldal,H.R. (1998). Summer distribution patterns and biomass estimates of macrozooplankton and micronekton in the Nordic Seas. *Sarsia*, 83,103-116.
- Foote,K.G., Knudsen,H.P., Korneliussen,R.J., Nordbø,P.E. and Røang,K. (1991). Postprocessing system for echo sounder data. *J. Acoust. Soc. Am.*,90(1),37-47.
- Godø, O.R., Valdemarsen,J.W. and Engås,A. (1993). Comparison of efficiency of standard and experimental juvenile gadoid sampling trawls. *ICES mar. Sci. Symp.* 196:196-201.
- Hirche,H-J., Hagen,W., Mumm,N. and Richter, C. (1994) The Northeast Water Polynya, Greenland Sea III. Meso- and macrozooplankton distribution and production of dominant herbivorous copepods during spring. *Polar Biol.*,14:491-503
- Johansen, Ø., Rye,H., Melbye,A.G., Jensen, H.V., Serigstad, B. and T. Knutsen (2001) Deep Spill JIP. Experimental Discharges of Gas and Oil at Helland-Hansen – June 2000. Sintef Applied Chemistry, Technical Report. No. STF66 F01082, Pp. 1-159.
- Kaartvedt,S., Melle,W., Knutsen,T. and Skjoldal,H.R.S. (1996) Vertical distribution of fish and krill beneath water of varying optical properties. *Mar. Ecol. Progr. Ser.*,136,51-58.
- Melle,W., Kaartvedt,S.,Knutsen,T., Dalpadado,P. and Skjoldal,H.R. (1993). Acoustic visualization of large scale macroplankton and micronekton distributions across the Norwegian shelf and slope of the Norwegian Sea. *ICES Council meeting*, L:44:1-25.
- Melle,W., Serigstad,B. and Ellertsen,B. (2001) Environmental risk of deep water oil drilling – preliminary analysis. Report No. 1/2001. Institute of Marine Research, Center of Marine Environment. Pp. 1-50.
- Ona,E. and Traynor,J. (1990) Hull mounted, protruding transducer for improving echo integration in bad weather. *ICES Council meeting*,B:31:1-10.
- Rye, H. and Johansen, Ø. (1999a). Spredning av dispergert olje i vannmassene og eksponering på marine organismer. SINTEF Report, STF66 A99029, Trondheim, March 1999, 64 pp.

- Rye, H. and Johansen, Ø. (1999b) Oil spill contingency for deep water exploration. Report from Phase 1: Basis for oil spill contingency planning: An assessment of the expected oil spill behavior during a deepwater blowout off the Norwegian coast (Norwegian Sea), 1999, SINTEF).
- Serigstad, B., Johansen, R.I., Stenevik, E.K. and S. Mjøs, (1997). Effekter av Troll-olje på marine organismer i de frievannmasser. Spesiell fokus på hvordan dispergeringsmidler påvirker giftighet og influensområde. Ocean Climate A/S, Bergen, Rapp. SA 60474. ISBN 82-461-046-6.
- Simard, Y., de Ladurantaye, R. Therriault, J.-C. (1986). Aggregation of euphausiids along a coastal shelf in an upwelling environment. *Mar. Ecol. Prog. Ser.*, 32(2-3), 203-215.
- Simard, Y. and Mackas, D.L. (1989). Mesoscale aggregations of euphausiid sound scattering layers on the continental shelf of Vancouver Island. *Can. J. Fish. Aquat. Sci.*, 46(7), 1238-1247.
- Torgersen, T., Kaartvedt, S., Melle, W. and Knutsen, T. (1997). Large scale distribution of acoustical scattering layers at the Norwegian Sea continental shelf and the eastern Norwegian Sea. *Sarsia*, 82, 87-96.
- Valdemarsen, J.W. and Misund, O.A. (1995). Trawl designs and techniques used by Norwegian Research Vessels to sample fish in the pelagic zone. Pp. 135-144 in Høyen, A. (ed) : Precision and relevance of pre-recruit studies for fishery management related to fish stocks in the Barents Sea and adjacent. Proceedings of the sixth IMR-PINRO Symposium, Bergen, 14-17 June 1994.
- Wiborg, K.F. (1954). Investigations on zooplankton in coastal and offshore waters of western and north-western Norway with special reference to the copepods. *Fisk. Dir. Skr. Ser. HavUnders.* 11(1):1-246.
- Wiebe, P.H., Burt, K.H., Boyd, S.H., and Morton, A.W. 1976. A multiple opening/closing net and environmental sensing system for sampling zooplankton. *J. Mar. Res.*, 34, 313-326.
- Wiebe, P.H., Morton A.W., Bradley, A.M., Backus R.H., Craddock J.E., Barber V., Cowles T.J. & G.R. Flierl, 1985. New developments in the MOCNESS, an apparatus for sampling zooplankton and mikronekton. *Marine Biology*, 87, 313-323.
- Østvedt, O.J. (1955). Zooplankton investigations from weather ship M in the Norwegian Sea, 1948-1949. *Hvalråd. Skr.* 40:1-93.
- Østvedt, O.J. (1965). The migration of Norwegian herring to Icelandic waters and the environmental conditions in May-June, 1961-1964. *Fisk. Dir. Skr. Ser. HavUnders.* 13(8):29-47.

Acknowledgements

Thanks are due to Cortis Cooper (Chevron) and Arne Myhrvold (Statoil) who made this work possible as an additional contribution from the DeepSpill_2000 field experiment. Arild Sundfjord (NIVA) and Ronald Pedersen (IMR) are particularly thanked for their efforts with the bottom mounted Long Ranger 75 kHz ADCP during the preparative phase and during the field experiment. Øistein Johansen (SINTEF Applied Chemistry) is thanked for various discussions on the behavior and dynamics of oil and gas as it ascends from deep water to the surface region. Signe Johannesen (IMR) and Laura Rey (IMR) have been responsible for the laboratory analysis of the biological samples collected during the experiment.

Appendix I. Mesozooplankton as obtained with the Mocness.

MOC no 1	24-06-2000	St 486	Lat :	6459.57 N	Lon :	0501.35 E
Max depth [m]		700	495	402	302	201
Min depth [m]		495	402	302	201	100
Net #		1+2	3	4	5	6
Time [UTC]		13:35				
Species / group	Stage / length (mm)	Ant. m ⁻³				
Calanus finmarchicus	I+II	0	0	0	0	0
	III	0.10		0.60		0.26
	IV	2.19	3.06	11.47	2.01	1.29
	V	11.74	54.75	39.23	19.50	16.62
	VIf	0.20	0.77	1.21	0.29	0.52
	VIm	0	0	0	0.14	0
C. hyperboreus	I+II	0	0	0	0	0
	III+IV	0	0	0	0	0
	V	0.05	0.17	0.13	0	0.02
	VIf	0.07	0.19	0.11	0	0.02
	VIm	0	0	0	0	0
Metridia	I-III	0.05	2.30	5.43	0.57	0.39
	IV-V	0	13.40	8.45	4.59	0.52
	VI	0.80	2.30	9.05	3.73	0.26
Pseudocalanus	I-III	0	0	0	0	0.52
	IV-VI	0.55	1.53	1.21	2.29	4.38
Euchaeta	I-III	0	0.77	1.21	0.57	0.39
	IV-VI	0.10	0.53	0.53	0.11	0
Microcalanus		0.80	7.66	24.14	24.95	32.60
Oithona		1.15	1.91	5.43	6.31	10.44
Oncaea		0.65	0.77	0.60	0.29	0.26
Cyclopoida		0	0	0	0	0
Harpacticoida		0	0	0	0	0.06
Copepoda		0	0	0	0	0
Copepoda	egg	0.05	0.38		0.57	0.77
Copepod	nauplii	0	0.38	0.60	0	0.26
Ostrachoda		0	1.15	0.60	0	0.02
Cladocera		0	0	0	0	0
Hyperiidia		0	0	0	0.32	0.14
Decapoda	larvae	0	0	0	0	0.03
Tomopteris		0	0	0.02	0	0
Polychaeta		0	0.38	0	0	0
		0	0	0	0	0
Euphausiac.	egg	0	0	0	0	0
Euphausiac.	nauplii	0	0	0	0	0
Euphausiac.	calyptopis	0	0	0	0.14	0
Euphausiac.	furcilia	0.05	0.38	0.02	0.29	0.24
Thysanoessa inermis		0	0	0	0	0
T. longicaudata		0	0	0	0	0
T. raschii		0	0	0	0	0
Meganctiphanes norvegica		0	0	0	0	0
Limacina retroversa	<2	0	0	0	0.14	0
	>2	0	0	0	0	0
Clione limacina	<10	0	0	0	0	0
	>10	0	0	0	0	0
Bivalvia		0	0	0	0	0.13
Aglantha digitale	<10	0	0	0	0	0
	>10	0.02	0.07	0	0	0
Sarsia spp.	<10	0	0	0	0	0
	>10	0	0	0	0	0
Hydrozoa	<10	0	0	0	0	0
	>10	0	0	0	0	0
Siphonophora		0	0.02	0.04	0	0
Chaetognatha	<10	0	0.05	0.11	0	0
	10-20	0	1.01	1.04	1.43	0.03
	>20	0.10	0.86	0.91	0.86	0.03
Other species / groups						
Chiridius spp.		0	0.38	0.09	0	0
Candacia armata		0	0.38	0.30	0	0.13
Scolecithricella minor		0	0	0.30	0.29	0.26
Pleuromamma robusta		0	0	0	0.14	0.13
Acartia longiremis		0.05	0	0	0	0
Gastropoda	larvae	0	0	0.60	0	0
Total number of organisms		18.73	95.55	113.44	69.54	70.70

Appendix I continued.

MOC no 2	24-06-2000	St 487	Lat :	6457.45 N	Lon :	0456.33 E	Time:	17:57		
Max depth [m]		707	500	401	301	200	100	50	25	25
Min depth [m]		500	400	301	199	100	50	25	0	0
Net #		1	2	3	4	5	6	7	8	8
Species / group	Stage / length (mm)	Ant. m ⁻³								
Calanus finmarchicus	I	0	0	0	0	0	0	0	0	3.13
	II	0	0	0	0	0	0	0	0	3.13
	III	0	0	0	0	0	0	0	0	3.13
	IV	3.92	0.16	1.59	2.07	1.18	1.60	23.33	238.05	
	V	124.55	1.32	18.67	3.55	6.39	7.67	306.22	1393.86	
	VI	0.49	0.04	0.35	0.30	0.30	1.00	96.24	40.72	
	VIIm	0	0	0	0.10	0.05	0	2.92	3.13	
C. hyperboreus	I-II	0	0	0	0	0	0	0	0	0
	III	0	0	0	0.10	0.08	0	0	0	0
	IV	0.02	0	0	0	0	0	0	0	0
	V	0.26	0	0.10	0.01	0	0	0.05	0	0
	VI	0.12	0.01	0.09	0.05	0.01	0	0	0.05	0
	VIIm	0	0	0	0	0	0	0	0	0
Metridia	I-III	0.49	0.03	3.17	0.79	0	0.13	1.46	3.13	
	IV-V	1.47	0.01	5.81	3.75	2.00	1.00	4.37	0	
	VI	0.38	0.06	5.11	10.26	0.80	0.07	0	0	
Pseudocalanus	I-III	0.49	0	0	0	0	0	0	0	0
	IV-VI	0.98	0.06	0.53	1.78	5.61	6.93	10.21	109.63	
Euchaeta	I-III	0.98	0	0.04	0.20	0.80	0.67	0	0	0
	IV-VI	0.44	0.03	0.11	0.12	0.03	0.07	0.09	0.05	
Microcalanus		5.88	0.68	10.57	16.37	63.34	8.00	0	6.26	
Oithona		0.98	0.39	5.11	6.31	5.21	56.00	650.35	106.50	
Oncaea		7.85	0.07	0.70	1.48	0	1.60	1.46	3.13	
Harpacticoida		0	0.01	0.09	0	0	0.53	0	0	
Copepoda	egg	0	0	0	1.68	0	0	0	0	
	nauplii	0	0	0	0.10	0	0	2.92	0	
Ostrachoda		0.09	0.01	0.53	0.20	0	0	1.46	0	
Cladocera		0	0	0	0.10	0	0	0	0	
Parathemisto abyssorum	<10	0	0	0	0	0.25	0.22	0.18	0	
	10-20	0	0	0	0	0	0	0.05	0	
Hyperidea		0.25	0.01	0.04	0.17	0	0	0	0	
Natantia		0	0	0.01	0	0	0	0	0	
Decapoda	larvae	0	0	0	0	0	0.12	0.14	0	
Polychaeta		0	0.01	0	0	0	0	0	0	
Echinodermata		0	0	0	0.10	0	0	0	0	
Euphausiacea	egg	0	0	0	0.10	0	0.53	0	0	
	nauplii	0	0	0	0.10	0	0	0	0	
	calypt.	0	0	0	0.10	0	1.07	0	0	
	furcilia	0	0.03	0.02	0.30	0	0.38	1.59	0.39	
Thysanoessa inermis		0	0	0	0	0	0.03	0	0	
T. longicaudata		0	0	0	0	0.03	0.32	0	0	
Meganctiphanes norvegica		0	0.01	0	0	0	0.05	0	0	
Euphausiacea		0	0	0	0	0	0.02	0	0	
Limacina retroversa	<2	0	0	0	0	0	0	0	6.26	
	>2	0	0	0	0	0	0	1.46	0	
Bivalvia		0	0	0	0	0	0.53	0	3.13	
Aglantha digitale	<10	0.05	0.01	0	0.05	0	0	0	0	
	>10	0.15	0.01	0	0	0	0	0	0	
Siphonophora		0	0.01	0.01	0.01	0	0	0	0	
Chaetognatha	<10	0	0	0	0.02	0	0	0.09	0.10	
	10-20	0	0	0.72	1.11	0.06	0	0.18	0.34	
	>20	1.16	0.02	0.30	0.46	0.01	0.03	0.09	0	
Acartia		0	0	0	0	0	0.53	2.92	15.66	
Heterohabdus norvegicus		0.03	0	0.04	0.02	0	0	0	0	
Candacia		0	0	0.01	0	0	0	0	0	
Chiridius		0.12	0	0.04	0.01	0	0	0	0	
Pleuromamma robusta		0	0.01	0.00	0.01	0	0	0	0	
Scolecithricella minor		0	0	0	0.20	0.40	0	2.92	0	
Isopod		0	0	0	0.10	0.40	0	0	0	
Ætidius armatus		0	0	0	0.05	0	0	0	0	
Anomalocera patersoni		0	0	0	0	0	0.07	0	0	
Total number of individuals		151.16	3.04	53.77	52.21	86.95	89.17	1110.69	1939.80	

Appendix I continued.

MOC no 3	29-06-2000	-	Lat :	6458.31 N	Lon :	0500.50 E	Time:	17:08		
Max depth [m]	700	500	400	300	200	100	50	25	25	
Min depth [m]	500	400	300	200	100	50	25	0	0	
Net #	1	2	3	4	5	6	7	8		
Species / group	Stage / length (mm)	Nos m-3	Nos m-3	Nos m-3	Nos m-3	Nos m-3	Nos m-3	Nos m-3	Nos m-3	Nos m-3
Calanus finmarchicus	I+II	0	0	0	0	0	0	0	0	0
	III	0	0	0	0	0	0	0	0	0
	IV	11.44	0.22	1.85	1.26	1.42	1.91	0	34.61	
	V	91.28	2.04	11.04	9.86	9.53	15.75	1194.22	1040.15	
	VI	2.45	0.03	0.22	0.12	0.38	0.83	83.76	3.85	
	VIIm	0.27	0	0	0.12	0	0.17	0	0	
C. hyperboreus	I+II	0	0	0	0	0	0	0	0	
	III	0.27	0	0.27	0	0.19	0.02	0	0	
	IV	0	0	0	0	0	0	0	0	
	V	0.18	0	0.04	0.02	0.01	0.01	0	0.03	
	VI	0.12	0	0.05	0	0.01	0	0	0	
	VIIm	0	0	0	0	0	0	0	0	
Metridia	I-III	0.54	0.07	1.90	1.80	0.38	0	0	1.92	
	IV-V	1.63	0.05	0.98	1.92	7.17	0.50	0	0	
	VI	4.90	0.07	0.87	0.48	8.87	0.58	0	0	
Pseudocalanus	I-III	0.00	0.01	0	0	0	0.33	0	1.92	
	IV-VI	1.09	0.06	1.41	2.64	1.13	6.63	2.70	44.22	
Euchaeta	I-III	0.27	0.01	0.43	0.12	1.32	0.99	0	0	
	IV-VI	0.13	0.03	0.05	0.02	0.21	0.06	0	0	
Microcalanus		0.27	0.10	1.90	6.25	14.16	28.85	0	1.92	
Calanoida		0	0	0.05	0	0	0	0	0	
Oithona		1.09	0.19	2	7.21	5.66	88.55	172.92	32.68	
Oncaea		11.44	0.17	1.09	1.68	1.32	4.64	0	3.85	
Cyclopoida		0.27	0.01	0.05	0	0	0	0	0	
Harpacticoida		0	0.02	0.11	0.12	0	0	0	0	
Copepod-nauplii		0	0.01	0	0	0	1.33	0	0	
Ostrachoda		0.03	0.01	0.33	0.48	0	0	0	0	
Parathemisto abyssorum	<10	0.03	0.01	0.01	0.02	0.21	0.32	0.51	0.03	
	10-20	0.01	0	0	0	0	0	0	0	
	>20	0	0	0	0	0	0	0	0	
Decapoda larvae		0	0	0	0	0	0	0.13	0	
Tomopteris		0	0	0.01	0.05	0	0	0	0	
Polychaeta		0	0.01	0	0	0	0	2.70	0	
Euphausiacea	egg	0	0	0	0	0	0	0	0	
Euphausiacea	nauplii	0	0	0	0	0	0	0	0	
Euphausiacea	calypt.	0	0	0.05	0	0	0	0	0	
Euphausiacea	furcilia	0.27	0.02	0.01	0	0.01	0.09	0.55	0.33	
Thysanoessa inermis	<10	0	0	0	0	0	0	0.08	0	
T. longicaudata	<10	0	0	0	0	0	0	0	0	
	11-15	0	0	0.01	0.02	0.01	0.02	0.21	0	
	>16	0	0	0	0	0	0.01	0	0	
Meganyctiphanes norvegica	<10	0	0	0	0	0	0.02	0	0	
	11-15	0	0	0	0	0.01	0.04	0	0	
	16-20	0	0	0	0	0	0.02	0	0	
	>20	0	0	0	0	0	0	0	0	
Euphausiacea	<10	0	0	0	0	0.01	0	0.08	0	
	>10	0	0	0	0	0.01	0.01	0	0	
Limacina retroversa		0	0	0	0	0	0	2.70	0	
Bivalvia		0	0.01	0	0	0.38	0	0	3.85	
Hydrozoa	<10	0.03	0.01	0.03	0.02	0.01	0.00	0	0	
	>10	0.07	0	0.01	0	0	0	0	0	
Siphonophora		0.01	0	0.01	0	0	0	0	0	
Chaetognatha	<10	0	0.01	0.07	0.26	0.05	0.03	0.04	0.06	
	10-20	0.03	0	0.41	0.43	0.27	0.25	0.55	0.09	
	>20	0.49	0.03	0.18	0.16	0.12	0.12	0.13	0	
Other species / groups										
Gaetanus brev.		0.02	0	0.01	0.01	0.01	0	0	0	
Heterorhabdus norvegicus		0.27	0	0.01	0	0.01	0	0	0	
Chiridius obt.		0.02	0	0.01	0	0	0	0	0	
Isopod		0.00	0.01	0	0.12	0	0.33	0	0	
Scolecithricella minor		0.54	0.01	0.11	0.24	0.19	0.99	0	0	
Pleuromamma robusta		0	0	0	0.12	0	0	0	0	
Acartia		0	0.01	0	0	0	0	2.70	9.61	
Temora		0	0	0	0	0	0	0	1.92	
Sebastes larvae		0	0	0	0	0	0	0.04	0.06	
Total number of organisms		129.50	3.24	25.83	35.56	53.04	153.40	1464.02	1181.10	

Appendix II. Meso zooplankton as obtained with Multinet

St 494 27.06.2000						St 496 28.06.2000					
Time [UTC] : 15:42		Position: 6459.02 N 0453.32 E				Time [UTC] : 15:51		Position: 6500.65 N 0452.18 E			
Max depth [m]	800	700	500	300	100	800	700	500	300	100	
Min depth [m]	700	500	300	100	0	700	500	300	100	0	
Net #	1	2	3	4	5	1	2	3	4	5	
Species / group	Stage /					Stage /					
	length [mm]	No m ⁻³	No m ⁻³	No m ⁻³	No m ⁻³	No m ⁻³	No m ⁻³	No m ⁻³	No m ⁻³	No m ⁻³	
Calanus finmarchicus	I	0	0	0	0	0	0	0	0	0	
	II	0	0	0.08	0	0	0	0	0	0	
	III	0	0	0	0.08	3.84	0	0	0.02	0	
	IV	5.12	8.00	1.68	2.32	21.76	9.60	1.92	0.26	0.90	
	V	123.20	64.96	19.36	8.60	334.08	137.60	38.40	5.04	4.54	
	VIf	1.60	0.64	0.32	0.80	11.52	3.20	0.48	0.04	0.24	
C. hyperboreus	VIm	0	0	0	0.12	1.28	0	0	0	0.02	
	I	0	0	0	0	0	0	0	0	0	
	II	0	0	0	0	0	0	0	0	0	
	III	0	0.32	0	0.16	0	0	0	0	0	
	IV	0	0	0	0	0	0.96	0	0	0	
	V	0	0.08	0.16	0	0	2.40	0	0	0	
Metridia	VIf	0.32	0.04	0.08	0	0	1.28	0.20	0.02	0.04	
	VIm	0	0	0	0	0	0	0	0	0	
	I-III	0	0.64	0.16	0	2.56	0	0.32	0.16	0.02	
Pseudocalanus	IV-V	7.68	1.28	6.64	2.48	0	0.64	1.6	0.32	2.08	
	VI	16.32	4.80	6.72	5.76	1.28	1.28	2.24	0.58	3.36	
Euchaeta	I-III	0.32	0	0	0	0	0	0	0.02	0	
	IV-VI	0.32	0.32	0.16	2.24	11.52	0	0	0.02	0.04	
Microcalanus	I-III	0	0.32	0.08	0.16	0	0	0	0.02	0.08	
	IV-VI	1.12	0.16	0.24	0.12	1.28	0.40	0.20	0.04	0.20	
Calanoida	0.96	0.32	0.32	5.52	5.12	0.32	2.72	0.18	0.16	0	
Oithona	0	0	0	0	0	0	0.16	0.02	0	0	
Oncaea	0.96	0.96	0.08	0.16	5.12	3.20	1.28	0.02	0.06	6.40	
Cyclopoida	0	0	0	0	0	0.32	0	0	0.04	0	
Harpacticoida	0	0	0	0	1.28	0	0	0	0	0	
Copepod-nauplii	0	0	0.08	0.24	1.28	0	0.48	0.02	0	0	
Ostracoda	0.16	0.32	0.16	0	0	0	0.32	0.12	0.04	0	
Cladocera	0	0.32	0	0	0	0	0	0	0	0	
Parathemisto abyssorum	<10	0.16	0.16	0	0.08	1.28	0.24	0.08	0	0.04	
	10-20	0.0	0	0	0	0	0	0.04	0	0	
	>20	0	0	0	0	0	0	0	0	0	
Polychaeta	0	0	0	0	0	0.32	0	0	0	0	
Euphausiacea	egg	0	0	0	0	0	0	0	0	0	
Euphausiacea	nauplii	0	0	0	0	0	0	0	0	0	
Euphausiacea	calypt.	0	0	0	0.08	0	0	0	0	0	
Euphausiacea	furcilia	0	0	0	0.04	1.28	0	0	0.02	0.40	
Thysanoessa longicauda	<10	0	0	0	0	0	0	0	0	0	
	11-15	0	0	0	0	0	0	0	0	0.08	
	>16	0	0	0	0	0	0	0	0	0	
T. raschii	<10	0	0	0	0	0	0	0	0	0	
	11-15	0	0	0	0	0	0	0	0	0.08	
	16-20	0	0	0	0	0	0	0	0	0	
	>20	0	0	0	0	0	0	0	0	0	
Limacina retroversa	<2	0	0	0	0.04	0	0	0	0	0	
	>2	0	0	0	0	0	0	0	0	0	
Bivalvia	0	0	0	0	2.56	0.32	0	0	0.02	1.28	
Hydrozoa	<10	0	0	0	0	0	0	0	0	0	
	>10	0	0.08	0	0	0	0.08	0	0	0	
Siphonophora	0	0.04	0	0	0	0	0	0	0	0	
Chaetognatha	<10	0	0	0.32	0	0	0	0	0.06	0.06	
	10-20	0	0.12	0.40	0.20	0	0	0.08	0.26	0.38	
	>20	0	0.32	0.24	0.04	0	0.56	0.40	0.04	0.02	
Other species / groups											
Chiridius obtusifrons	0	0.08	0	0.12	0	0	0	0.02	0	0	
Gaetanus brevispinus	0	0.04	0.08	0	0	0	0	0.04	0.06	0.02	
Anomalocera patersoni	0	0	0	0	0	0	0	0	0.02	0	
Ætidius armatus	0	0	0.16	0	0	0	0	0	0	0	
Heterorhabdus norvegicus	0	0	0	0	0	0.32	0	0.04	0	0	
Candacia armatus	0	0	0.16	0	0	0	0	0	0	0	
Temora spp.	0	0	0	0	0	0.32	0	0	0	0	
Scolecithricella minor	0	0.32	0.16	0.24	0	0	0	0	0	0	
Gastropod larvae	0	0	0	0	0	0	0	0.02	0	0	
Pleuromamma robusta	0	0	0.08	0.04	0	0	0	0	0	0	
Total number of organisms	159.2	86.6	39.4	34.8	547.8	163.7	51.3	7.9	12.9	597.7	

Appendix III. Mesozooplankton as obtained with the WP II net on 29 June 2000.

Station		501	1	501	2	501	3	501	4	501	5	501	6
Time [UTC]			08:09		08:35		08:58		09:26		10:52		11:14
Latitude			6500.03 N		6459.71 N		6459.24 N		6459.18 N		6459.85 N		6500.43 N
Longitude			0450.60 E		0450.67 E		0450.74 E		0451.33 E		0452.43 E		0452.90 E
Max depth [m]			100		100		100		100		100		100
Min depth [m]			0		0		0		0		0		0
Species / group	Stage / length [mm]		Nos m-3		Nos m-3		Nos m-3		Nos m-3		Nos m-3		Nos m-3
Calanus finmarchicus	I		3.84		2.56		0		2.56		0		0
	II		1.28		0		2.56		7.68		0		2.56
	III		6.40		5.12		5.12		2.56		0		0
	IV		35.84		35.84		33.28		25.6		23.04		28.16
	V		398.08		601.60		977.92		1128.96		657.92		616.96
	VI		24.32		28.16		17.92		25.60		40.96		25.60
	VI		0		0		2.56		2.56		2.56		2.56
Metridia	I-III		0		0		0		0		0		0
	IV-V		0		0		0		0		0		0
	VI		0		0		0		2.56		0		0
Pseudocalanus	I-III		10.24		7.68		25.60		20.48		10.24		12.80
	IV-VI		43.52		40.96		48.64		64		23.04		35.84
Euchaeta	I-III		1.28		0		0		0		0		0
	IV-VI		0.08		0		0		0		0		0
Microcalanus			1.28		0		0		23.04		2.56		20.48
Calanoida			0		0		0		0		0		0
Oithona			404.48		494.08		698.88		291.84		430.08		491.52
Oncaea			7.68		7.68		5.12		0		2.56		7.68
Copepoda	nauplii		19.20		2.56		5.12		5.12		7.68		2.56
Parthemisto abyssorum	<10		0.32		0.32		0.16		1.12		0.16		0.16
	10-20		0		0		0		0		0		0
	>20		0		0		0		0		0		0
Decapoda larvae			0		0		0.16		0		0		0
Euphausiacea	egg		0		0		0		0		0		0
Euphausiacea	nauplii		0		0		0		0		0		0
Euphausiacea	calyptopis		0		0		0		0		0		0
Euphausiacea	furcilia		0		0		12.80		12.80		0.32		0.16
Thysanoessa longicaudata	<10		0		0		0		0		0		0
	11-15		0		0.16		0		0		0.16		0
	>16		0		0		0		0		0		0
Limacina retroversa	<2		0		0		0		2.56		0		0
	>2		0		0		0		0		0		0
Clione limacina	<10		0		0		0		0		0		0
	>10		0.08		0		0		0		0		0
Bivalvia			1.28		2.56		0		0		5.12		2.56
Aglantha digitale	<10		0		0		0		0		0		0
	>10		0		0		0		0		0		0
Hydrozoa	<10		8.96		7.68		0.16		0		0		0.32
	>10		0		0		0		0		0		0
Chaetognatha	<10		0		0		0.16		0.16		0.32		0.48
	10-20		0		0.16		0.64		0.96		0.32		0
	>20		0		0		0		0		0		0
Other species / groups													
Acartia			6.40		2.56		12.8		5.12		0		10.24
Temora			1.28		0		0		0		0		5.12
Limacina			0		0		0		0		0		2.56
Scolecithricella minor			0		0		2.56		0		0		0
Cyphonautes larvae			0		2.56		0		0		0		0
Total number of organisms			975.84		1242.24		1852.16		1625.28		1207.04		1268.32

Appendix IV. Overview of samples collected for chemical and biomarker response analyses

Station	Date	Time	Pos N	Pos E	Gear	Matrix	Depth [m]	Chemistry	Nos	N ₂	Nos
496	28-06-2000	16:52	6501.24	0452.42	WP-II	Calanus	200-0	x	1		
497	28-06-2000	18:19	6501.18	0446.49	WP-II	Calanus	200-0	x	1		
498	28-06-2000	21:57	6458.50	0446.14	WP-II	Calanus	200-0	x	1		
499	28-06-2000	23:13	6458.49	0452.95	WP-II	Calanus	200-0	x	1		
501-1	29-06-2000	08:21	6500.15	0450.69	WP-II	Calanus	100-0	x	1	x	2
501-2	29-06-2000	08:44	6459.75	0450.56	WP-II	Calanus	100-0	x	1	x	2
501-3	29-06-2000	09:16	6459.24	0450.75	WP-II	Calanus	100-0	x	1	x	2
501-4	29-06-2000	09:41	6459.27	0451.48	WP-II	Calanus	100-0	x	1	x	2
501-5	29-06-2000	11:01	6459.92	0452.46	WP-II	Calanus	100-0	x	1	x	2
501-6	29-06-2000	11:22	6500.49	0452.89	WP-II	Calanus	100-0	x	1	x	2
501-7	29-06-2000	18:27	6459.74	0455.80	WP-II	Calanus	100-0	x	1	x	2
220	29-06-2000	20:43	6441.66	0522.77	WP-II	Calanus	100-0	x	1	x	4
486	24-06-2000	15:03	6456.94	0502.99	Mocness	Calanus	700-300	x	1		
486	24-06-2000	15:03	6456.94	0502.99	Mocness	Calanus	300-50	x	1		
487	24-06-2000	18:08	6457.57	0455.43	Mocness	Calanus	700-500	x	1		
487	24-06-2000	18:08	6457.57	0455.43	Mocness	Calanus	400-100	x	1		
487	24-06-2000	18:08	6457.57	0455.43	Mocness	Calanus	50-25	x	1		
487	24-06-2000	18:08	6457.57	0455.43	Mocness	Calanus	25-0	x	1		
Moc-3	29-06-2000	17:08	6458.31	0500.50	Mocness	Calanus	700-500	x	1	x	2
Moc-3	29-06-2000	17:08	6458.31	0500.50	Mocness	Calanus	300-100	x	1	x	2
Moc-3	29-06-2000	17:08	6458.31	0500.50	Mocness	Calanus	50-25	x	2	x	2
Moc-3	29-06-2000	17:08	6458.31	0500.50	Mocness	Calanus	25-0	x	2	x	2
Moc-3	29-06-2000	17:08	6458.31	0500.50	Mocness	Calanus	700-0	x	4	x	2
494	27-06-2000	16:10	6459.01	0453.34	Multinet	Calanus	800-700+ 100-0	x	1		
Tr 203	24-06-2000	07:37	6458.80	0500.42	Harstadtrawl	Krill	500	x	1		
Tr 203	24-06-2000	07:37	6458.80	0500.42	Harstadtrawl	Benthosema	500	x	1		
Tr 205	24-06-2000	12:07	6500.12	0501.47	Akratrawl	0-group haddock	30-0	x	1		
Tr 206	27-06-2000	19:31	6502.07	0450.49	Harstadtrawl	Benthosema	500	x	1		
Tr 208	29-06-2000	16:17	6458.68	0457.10	Akratrawl	0-group haddock	30-0	x	1		
488	26-06-2000	15:23	6459.14	0451.01	CTD	Water	500	x	1		
492	27-06-2000	08:58	6500.31	0450.24	CTD	Water	140	x	1		
493	27-06-2000	12:46	6500.45	0449.75	CTD	Water	200	x	1		
500	29-06-2000	06:05	6459.92	0450.19	CTD	Water	400	x	1		
501	29-06-2000	07:40	6500.01	0450.96	CTD	Water	100	x	1		
501	29-06-2000	07:40	6500.01	0450.96	CTD	Water	250	x	1		

